Pergamon

Geochimica et Cosmochimica Acta, Vol. 68, No. 3, pp. 591–606, 2004

0016-7037/04 $30.00 + .00

doi:10.1016/S0016-7037(03)00481-2

# The structural role of Ti in aluminosilicate liquids in the glass transition range: Insights from heat capacity and shear viscosity measurements

MATHIEU ROSKOSZ,[1,*] M. J. TOPLIS,[1] and PASCAL RICHET[2]

[1]Centre de Recherches Pétrographiques et Géochimiques, CNRS UPR 2300, 15 rue Notre-Dame des Pauvres, BP 20, 54501 Vandoeuvre-lès-Nancy Cedex, France

[2]Laboratoire de Physique des Minéraux et des Magmas, UMR CNRS 7047, Institut de Physique du Globe, 4 Place Jussieu, 75252 Paris Cedex 05, France

(*Received March* 14, 2003; *accepted in revised form June* 3, 2003)

**Abstract**—The shear viscosities and 1 bar heat capacities of glasses and melts along the 67mol% silica isopleth in the system $SiO_2$-$Al_2O_3$-$Na_2O$-$TiO_2$ have been determined in the temperature ranges 780–1140 K and 305–1090 K respectively. Anomalous behaviour of both these properties is observed for compositions rich in $TiO_2$ and/or $Al_2O_3$, an observation attributed to liquid-liquid phase separation followed by anatase crystallization. For samples which do not show anomalous behaviour, it is found that the partial molar heat capacity of the $TiO_2$ component previously determined in Al-free compositions reproduces our heat capacities to within 1.3%. Viscosity data show that addition of $TiO_2$ tends to increase viscosity and melt fragility at constant temperature. Furthermore, heat capacity and viscosity data may be combined within the framework of the Adam-Gibbs theory to extract values of the configurational entropy of the liquids and qualitative estimates of the variation of the average energy barrier to viscous flow. Configurational entropy at 900K is inferred to decrease upon addition of $TiO_2$, in contrast to previous results from Al-free systems. The compositional limit separating normal from anomalous behaviour, as well as the data for homogenous melts have been used to constrain the structural role of Ti in these samples. Our data are consistent with a majority of Ti in five-fold coordination associated with a titanyl bond, in agreement with previous spectroscopic studies. Furthermore, we find no evidence for a Ti-Al interaction in our samples, and we are led to the conclusion that Al and Ti are incompletely mixed, a hypothesis consistent with the observed reduction of configurational entropy upon addition of $TiO_2$, suggesting an important role of medium range order in controlling the variations in thermodynamic properties. 

## 1. INTRODUCTION

Titanium commonly occurs at the wt% level in natural terrestrial and extraterrestrial glasses, reaching concentrations as high as 16wt% $TiO_2$ in some lunar picrites (Longhi, 1992). Modeling the evolution of magmatic systems (*e.g.* solid-liquid phase equilibria, role of convection) therefore requires quantification of the influence of titania on the physical and thermodynamic properties of silicate melts. Early work on Ti-bearing liquids was interpreted to suggest that the structural role of titanium in silicate melts is a complex function of temperature and melt chemistry. For example, the partial molar volume of $TiO_2$ depends markedly on the nature of the alkali or alkaline-earth elements present in the melt (Dingwell, 1992 a; Liu and Lange, 2001), contrasting with the additive nature of volume-composition relationships generally observed for molten silicates (Lange and Carmichael, 1987; Bottinga and Weill, 1970). Furthermore, the heat capacity increase associated with the glass transition of Ti-rich glasses is unusually high, and followed by a strong decrease upon further heating (Richet and Bottinga, 1985; Lange and Navrotsky, 1993). In more recent years, spectroscopic methods have been employed to shed light on the structural origins for the 'anomalous' behaviour of Ti-bearing melts. Based upon these studies, a consensus is emerging that $Ti^{4+}$ is predominantly five-fold coordinated, associated with at least one low field strength metal cation. Four and six-fold coordination states may also be present, in abundances that are a function of composition but not temperature (Henderson and Fleet, 1995; Farges et al., 1996 a, b; Reynard and Webb, 1998; Henderson et al., 2002; Romano et al., 2000; Kroeker et al., 2002).

However, to date, most of the studies of Ti-bearing compositions have concentrated on addition of Ti to binary $M_nO$-$SiO_2$ glasses and liquids (where M is an alkali or alklaine earth cation), and application of these results to the chemically complex melts encountered in nature is questionable. In this respect, it is of particular note that Al, a major constituent of natural magmas, requires charge compensating cations to stabilise it in the liquid framework (Mysen, 1988). Thus, Al and Ti will be in competition for available low field strength cations and the presence of Al may significantly affect the role of titanium. This question has been addressed by Romano et al. (2000) from a spectroscopic point of view, but no studies of the role of Ti on physical and thermodynamic properties of Al-bearing silicate melts have been reported in the literature.

We have therefore chosen to investigate the variation of viscosity and heat capacity as a function of Ti content in the presence of variable amounts of Al. In this way, we also provide indirect evidence for the structural interactions between these two key elements and their interaction with other metal cations. Interest in alkali aluminosilicates also stems from the availability of spectroscopic data for similar compositions (Romano et al., 2000). In addition, melts in this system

* Author to whom correspondence should be addressed (roskosz@crpg.cnrs-nancy.fr).

Table 1. Chemical compositions (mol%[a]) of the investigated melts.

| | $SiO_2$ | $Na_2O$ | $Al_2O_3$ | $TiO_2$ | Na/(Na + Al) | molar mass | g atom[b] | $\rho$ (g/cm$^3$)[c] |
|---|---|---|---|---|---|---|---|---|
| NATS 70–0 | 67.17 | 23.00 | 9.79 | 0.00 | 0.701 | 64.627 | 3.196 | 2.464 |
| NATS 70–2 | 65.96 | 22.54 | 9.75 | 1.75 | 0.698 | 64.940 | 3.195 | 2.484 |
| NATS 70–4 | 64.53 | 22.48 | 9.48 | 3.50 | 0.703 | 65.175 | 3.190 | 2.503 |
| NATS 70–6 | 63.72 | 21.66 | 9.33 | 5.29 | 0.699 | 65.449 | 3.187 | 2.523 |
| NATS 70–8 | 62.40 | 21.37 | 9.04 | 7.19 | 0.703 | 65.699 | 3.181 | 2.541 |
| NATS 70–10 | 61.39 | 20.62 | 8.97 | 9.02 | 0.697 | 66.017 | 3.179 | 2.562 |
| NATS 58–0 | 66.34 | 19.74 | 13.89 | 0.00 | 0.587 | 66.283 | 3.278 | 2.439 |
| NATS 58–4 | 64.48 | 18.72 | 13.41 | 3.40 | 0.583 | 66.727 | 3.268 | 2.474 |
| NATS 58–8 | 62.97 | 17.27 | 12.90 | 6.86 | 0.572 | 67.173 | 3.258 | 2.504 |
| NATS 58–10 | 61.33 | 17.48 | 12.59 | 8.60 | 0.581 | 67.390 | 3.252 | 2.523 |
| NATS 58–11 | 60.74 | 17.19 | 12.54 | 9.53 | 0.578 | 67.546 | 3.251 | — |
| NATS 58–12 | 60.32 | 17.03 | 12.26 | 10.38 | 0.581 | 67.597 | 3.245 | — |
| NATS 54–0 | 66.89 | 18.21 | 14.81 | 0.00 | 0.552 | 66.649 | 3.296 | — |
| NATS 54–3 | 65.29 | 17.66 | 14.61 | 2.43 | 0.547 | 67.020 | 3.292 | — |
| NATS 54–6 | 63.64 | 17.14 | 14.16 | 5.05 | 0.548 | 67.341 | 3.283 | — |
| NATS 54–9 | 61.99 | 16.40 | 13.90 | 7.71 | 0.541 | 67.742 | 3.278 | — |
| NATS 54–12 | 60.53 | 16.05 | 13.38 | 10.05 | 0.545 | 67.978 | 3.268 | — |
| NATS 54–15 | 58.11 | 15.49 | 12.90 | 13.50 | 0.546 | 68.452 | 3.258 | — |
| NATS 50–0 | 66.17 | 17.07 | 16.69 | 0.00 | 0.506 | 67.412 | 3.334 | — |
| NATS 50–2 | 64.79 | 16.87 | 16.76 | 1.58 | 0.502 | 67.735 | 3.335 | — |
| NATS 50–4 | 64.15 | 16.12 | 16.05 | 3.69 | 0.501 | 67.840 | 3.321 | — |
| NATS 50–6 | 63.01 | 15.81 | 15.79 | 5.39 | 0.500 | 68.062 | 3.316 | — |
| NATS 50–8 | 61.98 | 15.41 | 15.36 | 7.26 | 0.501 | 68.244 | 3.307 | — |
| NATS 50–10 | 60.47 | 15.05 | 15.24 | 9.24 | 0.497 | 68.579 | 3.305 | — |

[a] Average of 10 analyses made with an electron microprobe.
[b] Number of atoms per gram of formula weight.
[c] Room-temperature Archimedean density of the glass.

can be easily supercooled permitting measurements over large temperature intervals (but see also below).

## 2. EXPERIMENTAL METHODS

### 2.1. Starting Compositions and Sample Preparation

Four base compositions in the ternary $SiO_2$-$Al_2O_3$-$Na_2O$ were studied. Each one contains 67 mol% $SiO_2$ and has molar $Na_2O/(Al_2O_3 + Na_2O)$ in the range 0.5 (the metaluminous join) to 0.7 (peralkaline). Large batches (approx. 300g) of these endmember glasses were synthesised from mixtures of reagent grade oxides ($SiO_2$, $Al_2O_3$) and carbonates ($Na_2CO_3$) melted at 1600°C in a thin walled Pt-crucible for periods of several hours. These glasses were crushed and remelted to ensure chemical homogeneity. Additions of up to 15 mol% $TiO_2$ (added as $TiO_2$) were made to these base compositions, such that $TiO_2$ was the only compositional variable at constant $Na_2O/(Al_2O_3 + Na_2O)$. Approximately 50g of each Ti-bearing composition was mechanically homogenised for periods of up to 10 hours during concentric cylinder viscosity measurements at temperatures in the range 1640 to 1000°C (Toplis and Dingwell, 1995). The compositions of glass chips recovered after these viscosity measurements were determined by electron microprobe and are shown in Table 1. Using analytical conditions of 10nA, 15kV and an incident beam diameter of 5 microns, measured Na/Al was observed to be a function of titanium content, an effect most marked in the most peralkaline series. Ten sequential analyses of the same spot showed this to be an artefact due to progressive sodium loss under the electron beam. Analyses performed using a beam current of 8nA and a defocussed beam of 20 microns showed no dependence of measured Na/Al on $TiO_2$ content, implying that sodium loss was negligible under these conditions. All the samples used for this study were taken from the large cylinders of glass recovered from the concentric cylinder viscosity measurements.

### 2.2. Heat Capacity Measurements

Heat capacities have been measured from room temperature to 1100K with a Setaram DSC 121 (Differential Scanning Calorimetry) under an argon-gas flow of 15 ml/h and crystalline $Al_2O_3$ as an internal standard. Full details of the experimental procedure are given in Linard et al., (2001). All measurements have been performed in step-scanning mode, in intervals of 25 K with a heating rate of 3 K/min and a time delay of 600s. Additional measurements were made for selected compositions every 10 K with a heating rate of 1K/min and a time delay of 400s in order to increase the number of experimental data points in the temperature range corresponding to the liquid state. The results obtained using the shorter time delay gave identical results, indicating that measurements correspond to fully relaxed liquid. Although measurements made near the glass transition may correspond to incompletely relaxed liquid, the stepwise nature of the measurements avoids the peak in heat capacity associated with continuous scanning.

### 2.3. Viscosity Measurements

Viscosities in the range $10^9$ to $10^{13}$ Pa.s have been measured in air under uniaxial compression with inaccuracies lower than 0.04 log units, as determined from measurements on NBS standard glass 710, with the setup described by Neuville and Richet (1991). The deformation rate is measured as a function of the stress applied at constant temperature. The samples were typically small cylinders 5 mm in diameter and 10 mm in height. From measurements of the sample height as a function of time, the viscosity of the melt was calculated by:

$$\eta = \frac{\sigma}{3\Delta 1\mathrm{n}\, L/\Delta t} \quad (1)$$

where $\sigma$ is the stress exerted, $L$ is the height of the sample and $t$ is time. For almost all compositions, measurements were made on several samples. Samples were randomly heated or cooled to final temperature. At a given temperature, the stress was varied to check the Newtonian nature of the viscosity. Sipp (1998) and Bouhifd et al. (1999) have found that, at viscosities higher than $10^{12}$ Pa.s, titanium-bearing silicate melts reach the equilibrium state seven to ten times more slowly than their titanium-free counterparts at the same viscosity. Therefore, care was taken to ensure that the rate of length change once the stress had been applied, was time independent. For Ti-rich compositions at low

Table 2. Log (Viscosity) in Pa.s.

| T (K) | 70:0 | T (K) | 70:2 | T (K) | 70:4 | T (K) | 70:6 | T (K) | 70:8 | T (K) | 70:10 |
|---|---|---|---|---|---|---|---|---|---|---|---|
| 781.07 | 13.10 | 813.15 | 12.32 | 814.99 | 12.78 | 834.91 | 12.40 | 834.51 | 13.08 | 856.88 | 12.43 |
| 802.18 | 12.12 | 828.85 | 11.58 | 819.19 | 12.59 | 850.76 | 11.60 | 850.96 | 12.09 | 867.71 | 11.75 |
| 818.19 | 11.42 | 845.32 | 10.90 | 835.71 | 11.81 | 866.73 | 10.87 | 867.03 | 11.29 | 879.4 | 11.05 |
| 834.02 | 10.79 | 861.52 | 10.31 | 851.35 | 11.10 | 882.53 | 10.21 | 882.82 | 10.56 | 889.76 | 10.53 |
| 855.11 | 10.04 | 877.73 | 9.77 | 867.42 | 10.45 | 898.63 | 9.68 | 898.82 | 9.90 | 899.99 | 10.09 |
| 871.75 | 9.56 | 888 | 9.50 | 883.6 | 9.90 | | | 909.4 | 9.54 | 910.08 | 9.70 |
| | | | | 899.31 | 9.43 | | | | | | |

| T (K) | 58:0 | T (K) | 58:4 | T (K) | 58:8 | T (K) | 58:10 |
|---|---|---|---|---|---|---|---|
| 887.5 | 12.05 | 897.6 | 12.42 | 905.9 | 12.1 | 909.6 | 12.43 |
| 903.4 | 11.48 | 913.6 | 11.75 | 916.9 | 11.65 | 925.5 | 11.79 |
| 919.4 | 10.95 | 929.4 | 11.13 | 927.6 | 11.21 | 941.3 | 11.18 |
| 940.6 | 10.32 | 945.0 | 10.58 | 938.4 | 10.79 | 957.2 | 10.61 |
| 961.9 | 9.76 | 961.5 | 10.05 | 956.4 | 10.21 | 972.5 | 10.14 |
| | | 977.5 | 9.63 | 961.4 | 10.04 | 988.5 | 9.63 |
| | | | | 971.0 | 9.75 | | |
| | | | | 982.5 | 9.41 | | |

| T (K) | 54:0 | T (K) | 54:3 | T (K) | 54:12 |
|---|---|---|---|---|---|
| 935.3 | 12.15 | 942.4 | 12.22 | 961.2 | 12.52 |
| 946.4 | 11.8 | 958.6 | 11.66 | 977.0 | 12.02 |
| 962.7 | 11.31 | 974.6 | 11.13 | 998.4 | 11.31 |
| 978.2 | 10.86 | 990.3 | 10.65 | 1014.4 | 10.78 |
| 994.1 | 10.43 | 1006.1 | 10.21 | 1030.2 | 10.3 |
| 1010.5 | 10.04 | 1022.2 | 9.82 | 1046.2 | 9.83 |
| 1026.4 | 9.71 | | | | |
| 1037.0 | 9.47 | | | | |

| T (K) | 50:0 | T (K) | 50:2 | T (K) | 50:4 | T (K) | 50:6 | T (K) | 50:8 | T (K) | 50:10 |
|---|---|---|---|---|---|---|---|---|---|---|---|
| 1026.8 | 12.5 | 1027.3 | 12.28 | 1028.2 | 12.53 | 1062.4 | 11.8 | 1057.7 | 11.9 | 1047.6 | 12.3 |
| 1047.5 | 11.93 | 1048.8 | 11.68 | 1039.0 | 12.23 | 1077.8 | 11.37 | 1071.9 | 11.43 | 1059.1 | 11.94 |
| 1063.3 | 11.5 | 1069.7 | 11.15 | 1049.4 | 11.95 | 1093.4 | 10.96 | 1088.0 | 10.99 | 1068.5 | 11.67 |
| 1079.0 | 11.1 | 1075.4 | 11.02 | 1070.1 | 11.39 | 1108.1 | 10.6 | 1103.7 | 10.61 | 1085.1 | 11.2 |
| 1095.1 | 10.75 | 1096.4 | 10.51 | 1091.4 | 10.84 | 1119.4 | 10.35 | 1119.4 | 10.23 | 1095.4 | 10.94 |
| 1115.7 | 10.3 | 1111.7 | 10.2 | 1111.9 | 10.33 | 1150.5 | 9.69 | 1135.2 | 9.87 | 1105.7 | 10.71 |
| 1136.1 | 9.89 | 1127.3 | 9.85 | 1127.4 | 9.95 | | | | | 1121.0 | 10.35 |
| | | | | 1142.7 | 9.65 | | | | | 1137.0 | 10.04 |

temperature, this time was on the order of several hours. The shape of the sample after viscosity measurements was still cylindrical indicating that no shearing occurred and that the linear approximation ($V$ = constant) is valid. No evidence for non-Newtonian behaviour was found except for samples from the series NATS 50 that contain 8 and 10 mol% $TiO_2$. For these compositions, the values of viscosity reported in Table 2 correspond to the measurements made under the maximum stress exerted. Using optical and scanning electron microscopy, no evidence for crystallization was observed after the measurements. Likewise, Archimedean densities of all samples were determined in a toluene bath before and after viscosity measurements. No significant changes were observed, with the exception of samples of the NATS 50 series.

## 3. RESULTS

### 3.1. Heat Capacity Measurements

The calorimetric measurements made between 305 and 1090 K are listed in Appendix 1 and plotted in Figure 1 for selected compositions. Data for the series NATS 50 are not included since the glass transition temperatures are above the range accessible by the Setaram DSC121. For the other cases, data for the glass phase has been fitted to an equation of the form:

$$C_p = a + bT + c/T^2 + d/T^{1/2}, \quad (2)$$

The same equation was adjusted to the data for the liquid phase with parameters b and d, or c and d set to zero. The values of the variables are listed in Table 3.

In the solid state, the heat capacity of all samples increases with increasing temperature until the glass transition is reached and a large increase in heat capacity is observed (Fig. 1). This jump in $C_p$ is observed to occur when the heat capacity of the glass is close to the Dulong and Petit harmonic limit of $3R/g$ atom ($R$ = gas constant), as observed in numerous previous studies of amorphous silicates (Haggerty et al., 1968; Richet and Bottinga, 1986; Toplis et al., 2001).

Above the glass transition, three different styles of variation of $C_p$ with temperature are observed. Firstly, for compositions with Na/(Na + Al) $>$ 0.5 containing little or no $TiO_2$, heat capacity is either independent of temperature or shows a slight positive temperature dependence. This behaviour is typical of aluminosilicate liquids (e.g. Stebbins et al., 1983; Richet and

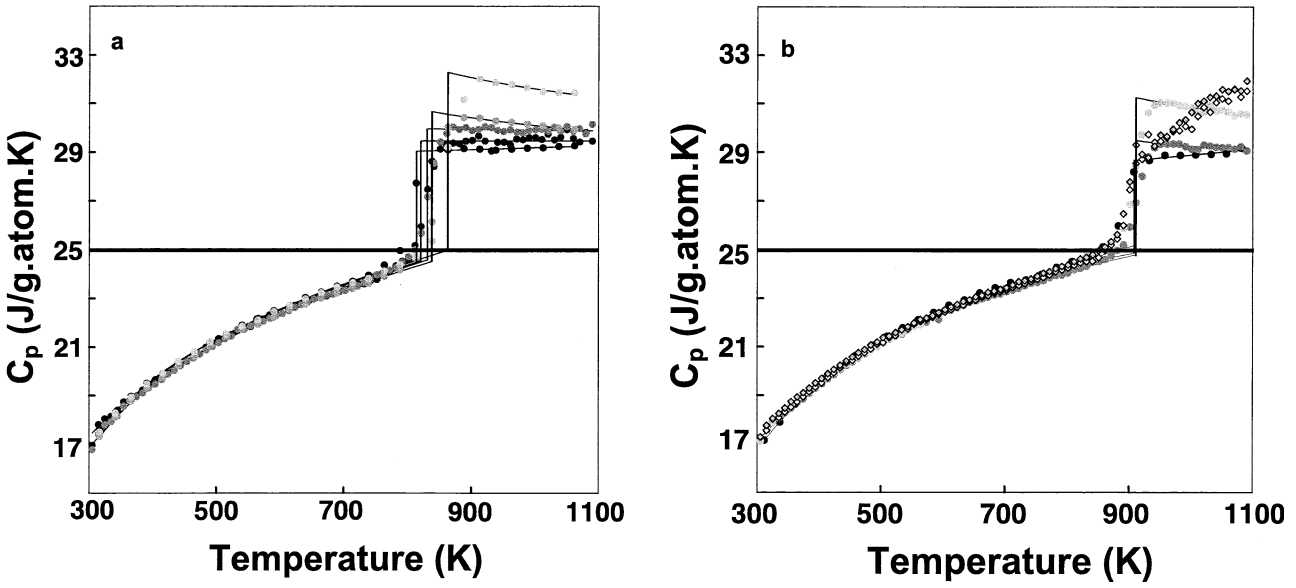


Fig. 1. Heat capacity of glasses and liquids of the series NATS 70 and NATS 58 as a function of absolute temperature. The solid line at ±25 *J/g.atom.K* represents the Dulong-Petit harmonic limit (*3R*) (a) NATS 70 : 0, 2, 4, 6, 10 (Circles black to light grey). (b) NATS 58 : 0, 4, 8 (Circles black to light grey) and NATS 58 : 10, 11 (open diamonds).

Bottinga, 1984; Richet and Neuville, 1992; Courtial and Richet, 1993), one notable exception being the data of Tangeman and Lange (1998) for sodium aluminosilicates, which show a slight negative temperature dependence. Secondly, for samples containing high concentrations of Ti, a clear negative dependence of $C_p$ on temperature is observed (Fig. 1). This behaviour is qualitatively similar to that described by other workers for simple alkali titanosilicate melts (Richet and Bottinga, 1985; Lange and Navrotsky, 1993; Tangeman and Lange, 1998; Bouhifd et al., 1999). In detail, for the series NATS 70 (Fig. 1a) for which the data are most comprehensive, the increase in heat capacity at the glass transition is found to be directly proportional to the $TiO_2$ content. We also note that, despite the increasingly large jump of $C_p$ at $T_g$, the heat capacity of the liquid markedly decreases with increasing temperature tending to the $C_p$ value of the analogous Ti-free melt (Fig. 1a). For the third type of variation, the change of $C_p$ at the glass transition is not as abrupt as expected. Furthermore, $C_p$ increases significantly in the liquid state and measurements are more scattered than usual (Fig. 1b). This type of variation is observed for those compositions richest in $TiO_2$ at Na/(Na + Al) = 0.58 and 0.54 as illustrated in Fig. 2, and discussed below.

For compositions which do not show the third type of behaviour, calorimetric glass transition temperatures $T_g$ have been defined as the temperature at which heat capacity is halfway between extrapolated values of fully relaxed liquid and completely unrelaxed glass. When defined in this way (Table), it is of note that Tg is within ±5 K of $T_{12}$, the temperature at which viscosity is $10^{12}$ Pa.s, as previously observed by Sipp and Richet, (2002).

### 3.2. Viscosity

The experimental viscosities are listed in Table 2 and shown in Figure 3. In general it is found that titania increases viscosity over the studied temperature ranges. For example, addition of 10 mol% $TiO_2$ to NATS 70:0 increases viscosity by more than two orders of magnitude at 860K, an increase which may be described as a linear function of $TiO_2$ (Fig. 4). However, with increasing temperature, the isothermal influence of $TiO_2$ on viscosity decreases (Fig. 4), consistent with previous observations that $TiO_2$ decreases viscosity in the superliquidus range (Dingwell, 1992 b; Bouhifd et al., 1999). We note that linearity may break down at higher $TiO_2$ contents as indicated by the observations of Dingwell (1992 b) and Bouhifd et al. (1999) for additions of up to 50 mol% $TiO_2$ to alumina-free melts. Some-

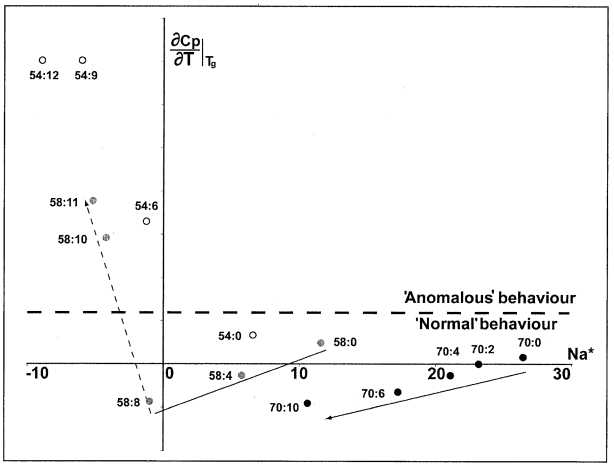


Fig. 2. Linear temperature dependence of heat capacities for fully relaxed liquids as a function of Na*, defined as molar *Na – Al – 1.4Ti* (see discussion for more details of this parameter). Black circles = NATS 70, Grey circles = NATS 58, Open circles = NATS 54. Below the dashed line, behaviour is considered 'normal' while above the dashed line, behaviour is 'abnormal.'

Table 3. Coefficients of $C_p = a + bT + c/T^2 + d/T^{1/2}$ ($C_p$ in J/molK).

| | | $a$ | $10^3 b$ | $10^{-}5c$ | $d$ | $\Delta T$[a] (K) | $T_g$ (K) | $AAD$[b] (%) | $AAD^c_{mod}$ (%) |
|---|---|---|---|---|---|---|---|---|---|
| NATS 70:0 | glass | 96.237 | 8.935 | −3.490 | −698.5 | 305–739 | 802 | 0.11 | 0.3 |
| | liquid | 90.751 | 2.515 | — | — | 863–1062 | | 0.09 | 0.09 |
| NATS 70:2 | glass | 85.474 | 15.004 | −3.033 | −541.8 | 305–802 | 820 | 0.40 | 1.0 |
| | liquid | 89.601 | 4.772 | — | — | 862–1041 | | 0.30 | 0.58 |
| NATS 70:4 | glass | 70.896 | 19.460 | −9.976 | −208.4 | 305–772 | 832 | 0.25 | 1.3 |
| | liquid | 94.948 | — | 4.400 | — | 882–1080 | | 0.21 | 0.56 |
| NATS 70:6 | glass | 62.295 | 21.251 | −1.393 | — | 305–789 | 841 | 0.15 | 1.3 |
| | liquid | 91.653 | — | 42.475 | — | 888–1062 | | 0.06 | 1.09 |
| NATS 70:10 | glass | 61.944 | 22.349 | −13.467 | — | 305–815 | 863 | 0.12 | 0.6 |
| | liquid | 94.082 | — | 63.578 | — | 913–1062 | | 0.08 | 0.87 |
| NATS 58:0 | glass | 134.865 | −8.863 | 1.804 | −1373.3 | 312–760 | 884 | 0.09 | 0.3 |
| | liquid | 86.852 | 7.840 | — | — | 933–1083 | | 0.20 | 0.19 |
| NATS 58:4 | glass | 123.86 | −1.161 | 5.279 | −1259.2 | 305–862 | 903 | 0.31 | 1.0 |
| | liquid | 94.462 | — | 20.159 | — | 951–1080 | | 0.21 | 0.57 |
| NATS 58:8 | glass | 95.030 | 11.321 | −2.625 | −686.1 | 305–822 | 907 | 0.14 | 0.7 |
| | liquid | 94.005 | — | 64.863 | — | 961–1090 | | 0.18 | 1.03 |
| NATS 54:0 | glass | 11.864 | 2.736 | 0.324 | −1048.3 | 312–834 | 934 | 0.14 | 1.3 |
| | liquid | 61.540 | 10.791 | — | — | 983–1083 | | 0.17 | 0.17 |

[a] Temperature interval of the measurements.
[b] Absolute average deviations of the experimental data from the fitted values.
[c] Absolute average deviations of the experimental data from the values calculated using Eq. 3 as discussed in the text.

what surprisingly, no variation of viscosity with $TiO_2$ content is found for the series NATS 50. However, as mentioned above, compositions NATS 50:8 and 50:10 show time dependent viscosity, and the significance of these latter observations will be discussed in the next section.

For compositions which do not show anomalous time or temperature dependence, viscosity data may also be used to calculate melt 'fragility,' a parameter used to quantify the departure from Arrhenian temperature dependence, defined by Angell (1985, 2001) as the gradient $\partial(log\eta)/\partial(T_g/T)$ at the glass transition temperature, $T_g$. We observe that fragility increases dramatically upon addition of 10 mol% $TiO_2$ to NATS 70:0. The magnitude of this effect is considerably greater than that due to equivalent additions of $Al_2O_3$ or $Na_2O$. However, in contrast to the variation of viscosity, fragility does not show a linear variation as a function of $TiO_2$ content. Melt fragility is also observed to increase for the other compositional series (Fig. 5), but the data do not cover a wide enough range of $TiO_2$ to assess whether the effect of titania on fragility is a function of $Al_2O_3$ content. For reference, we note that Bouhifd et al. (1999) showed that the fragility of Al-free alkali titanosilicate melts depends only on $TiO_2$ content and not on the abundance of $SiO_2$ or alkali elements.

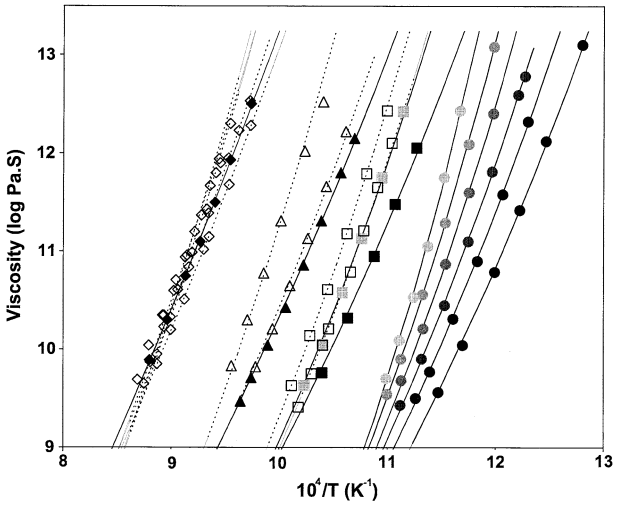


Fig. 3. Viscosity of aluminous titanosilicates as a function of reciprocal temperature. NATS 70-0, 2, 4, 6, 8, 10 = circles (black to light-grey respectively); NATS 58-0, 4 = black and grey squares respectively; NATS 58-8, 10 = open squares; NATS 54-0, 3, 12 = triangles (open for the last one); NATS 50-0, 2 = filled diamonds; NATS 50-4, 6, 8, 10 = open diamonds. Solid and dashed lines are fits to the TVF equation of data shown here and measurements in the superliquidus range (Toplis and Dingwell, unpublished data). Open symbols and dashed lines are used for data sets showing anomalous behaviour (see text).

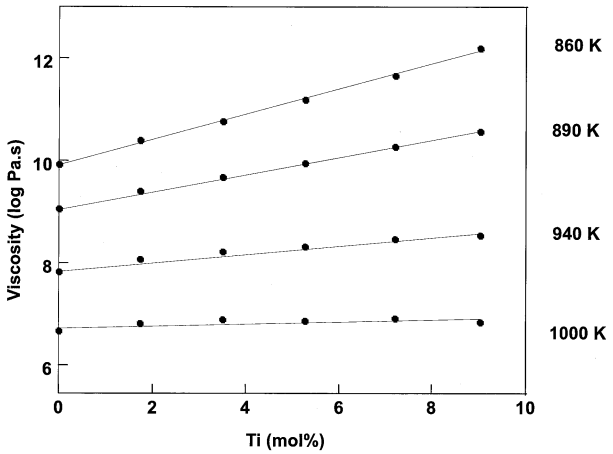


Fig. 4. Interpolated viscosity of NATS 70 as a function of titanium content at different temperatures.

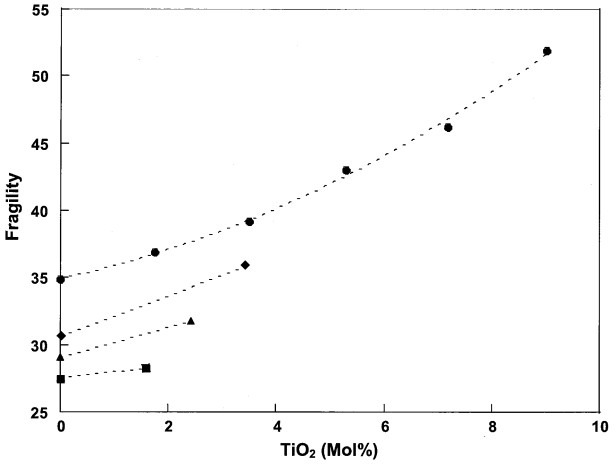


Fig. 5. Melt fragility as a function of titania content for samples not showing anomalous behaviour (full symbols on Fig. 3). Circles = NATS 70, diamonds = NATS 58, triangles = NATS 54, squares = NATS 50.

## 4. DISCUSSION

### 4.1. Processes Responsible for Anomalous Behaviour: Liquid-Liquid Phase Separation and Anatase Saturation

As noted above, unusual temperature dependence of $C_p$ and viscosity occurs for the same compositions. After heat capacity measurements (which typically lasted 6 h, of which only the last 2 were above the glass transition temperature) optical and electron microscopies (SEM, TEM) showed no evidence for partial crystallization. As crystallization is exothermic it cannot explain the observed variations of $C_p$. On the other hand, these variations are similar to those recently described in the system $Na_2O$-$SiO_2$ (Jarry and Richet, 2001), where they have been attributed to liquid-liquid unmixing (i.e. immiscibility). Indeed, unmixing is a process known to be promoted by the presence of Ti (Glasser and Maar, 1979). Furthermore, time-dependent viscosity measurements have been previously described in Ti-rich systems and ascribed to immiscibility (Simmons et al., 1974; Sipp et al., 1997). Transmission Electron Microscopy (TEM) performed on NATS 50:6 before viscometry was impaired by extremely rapid volatilization of sodium under the electron beam, but no features corresponding to crystals or immiscible phases were apparent. On the same sample, after viscosity measurements lasting approximately 7 h above the glass transition, volatilization of sodium under the electron beam was still problematic during observation by TEM, but in this case the sample also clearly contained nanocrystals, found to be anatase based upon Raman spectroscopy. Raman spectra of other samples showing anomalous behaviour also imply the presence of crystalline anatase. Our result that the viscosity of $TiO_2$-bearing melts in the series NATS 50 is similar to that of the $TiO_2$-free melt may therefore be explained because essentially all $TiO_2$ has been extracted from the liquid into anatase. Note that the volume fraction of these inclusions is too small to influence viscosity directly (Lejeune and Richet, 1995).

Although it cannot be proven that saturation of $TiO_2$ is the result of a preceding liquid-liquid immiscibility, some process is clearly active during the heat capacity measurements, but no crystals were observed in those samples, even at the scale of observation of the transmission electron microscope. Detailed consideration of the compositional domain where $TiO_2$ saturation occurs, and the implications for the structural role of $TiO_2$ in our glasses, will be presented below.

### 4.2. Influence of Titania on the Properties of Homogeneous Melts

#### *4.2.1. Partial molar heat capacities of oxide components*

For silicate glasses, it has long been known that heat capacity is an additive function of composition above room temperature (Stebbins et al., 1984; Richet, 1987). With oxide components one writes

$$C_p^{gl} = \sum \varkappa_i \bar{C}_{pi}, \tag{3}$$

where $\varkappa_i$ is the mole fraction and $\bar{C}_{pi}$ the partial molar heat capacity of oxide *i*. With the composition independent $\bar{C}_{pi}$'s of Richet (1987), we reproduce all measurements to better than 1.3% (Table 3).

In contrast, there is no universally applicable model for the prediction of liquid heat capacity. In order to simulate our experimental data, an additive model analogous to equation 3 has been used. Our first step is to assess whether temperature dependent values of $\bar{C}_{pTiO_2}$ determined from Al-free compositions (for which only Richet and Bottinga, 1985 provide a quantitative model) can be applied to our liquids. To test this we have calculated $\varkappa_{TiO_2} \cdot \bar{C}_{pTiO_2} + (1 - \varkappa_{TiO_2}) \cdot \bar{C}_{pTi\ -\ free}$ where $\bar{C}_{pTi\ -\ free}$ is the measured heat capacity of the Ti-free composition and $\bar{C}_{pTiO_2}$ is the value given by Richet and Bottinga (1985). The agreement between the predicted values of $C_p$ and experiments is better than 1% for all compositions not affected by immiscibility/crystallisation (Fig. 6). We therefore conclude that the partial molar heat capacity of $TiO_2$ determined in Al-free systems is also applicable to Al-bearing compositions.

Furthermore, even though many studies have shown that the partial molar heat capacity of $Na_2O$ and $SiO_2$ components are independent of temperature and composition (Stebbins et al., 1984; Lange and Navrotsky, 1992) the case for the $Al_2O_3$ component is known to be more complex (Richet and Bottinga, 1985; Courtial and Richet, 1993; Tangeman and Lange, 1998), thus we have considered in more detail the values of $\bar{C}_{pTi\ -\ free}$. In order to remain consistent with previous determinations of partial molar heat capacity determined from large data sets of precise measurements (in particular from drop calorimetry) we have chosen to impose $\bar{C}_{pNa_2O}$ and $\bar{C}_{pSiO_2}$ from Richet and Bottinga (1985), values identical within error to those of other models (*e.g.* Stebbins et al., 1984; Lange and Navrotsky, 1992). Values of $\bar{C}_{pAl_{2O3}}$ were then determined for each Ti-free composition. Despite the limited temperature range of our experiments, a temperature dependent $\bar{C}_{pAl_2O_3}$ was required to fit the data and an equation of the form $\bar{C}_{pAl_2O_3} = a + bT$ was used as in previous studies (Richet and Bottinga, 1984; Courtial and Richet, 1993). It is observed that the values of parameters *a* and *b* determined in this way vary as a linear function of the ratio $Na_2O/(Al_2O_3 + Na_2O)$ as summarized in Table 4.

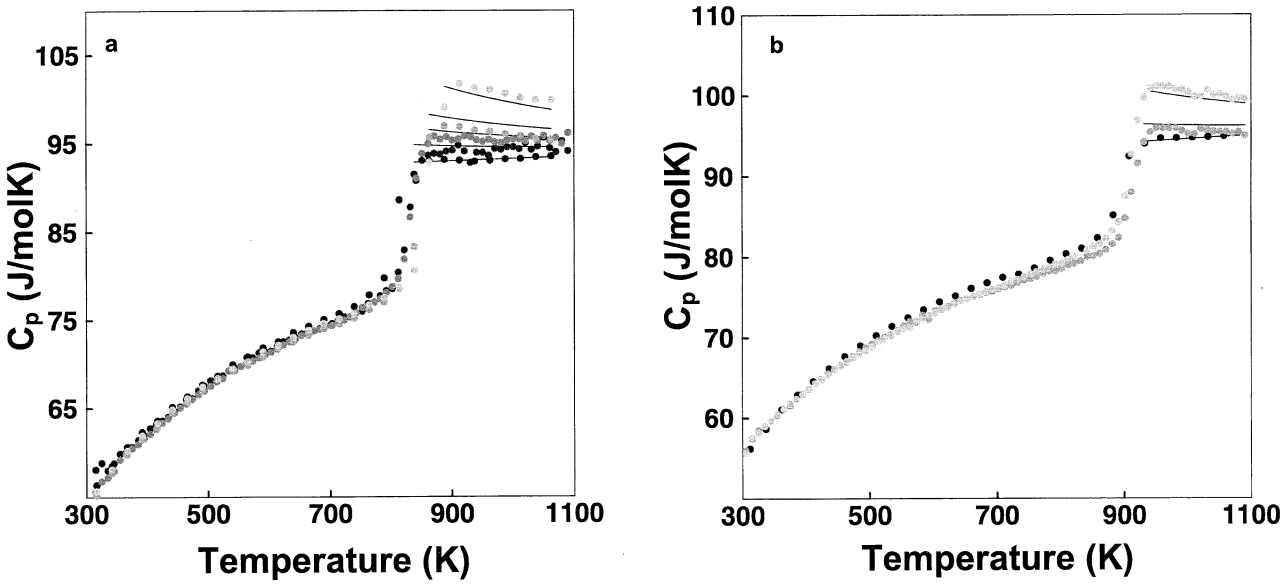


Fig. 6. Calculated heat capacities of the melts with the model described in the text (Eq. 3 and Table 3). (a) NATS 70 (b) NATS 58. Error bars are not presented but are less than 1% (see Table 3).

*4.2.2. Application of the Adam-Gibbs theory*

Within the framework of the Adam and Gibbs (A-G) theory of relaxation processes (Adam and Gibbs, 1965) it may be shown (Richet, 1984) that viscosity ($\eta$) of a liquid is related to its configurational entropy ($S^{conf}(T)$) through the equation

$$\log_{10}(\eta) = A_e + \frac{B_e}{TS^{conf}(T)}, \tag{4}$$

where $A_e$ and $B_e$ are constants. Using the glass transition temperature $T_g$ as an arbitrary reference temperature, we may write for $S^{conf}(T)$

$$S^{conf}(T) = S^{conf}(T_g) + \int_{T_g}^{T} \frac{C_p^{conf}}{T} dT, \tag{5}$$

In this equation $C_p^{conf}$ corresponds to the configurational contribution to liquid heat capacity, which is given by (Richet, 1984):

$$C_p^{conf} = C_p^{diq} - C_p^{vib}, \tag{6}$$

where $C_p^{vib}$ may be approximated by the composition independent value of 3R/g atom, corresponding to the heat capacity of the glass at $T_g$ (Haggerty et al., 1968, Richet and Bottinga, 1986). $C_p^{conf}$ is a parameter associated with temperature induced changes in the liquid, mainly controlled by short-range order around oxygen atoms (Richet and Bottinga, 1985). Defining $T_g$ in equation 5 as the temperature at which viscosity is $10^{12}$ Pas, equations 4 and 5 may be combined and fitted to available heat capacity and viscosity data using $S^{conf}(T_g)$, $A_e$ and $B_e$ as fit parameters. In this way our data may be used to provide further insights into the variation of thermodynamic properties as a function of $TiO_2$. Not only can we consider the variation of $S^{conf}(T_g)$, but also that of $B_e/S^{conf}$ $(T_g)$, a ratio proportional to the height of the average potential energy barrier to viscous flow (Toplis, 1998).

Table 4. Coefficients $a$ and $b$ of $\bar{C}_{pAl_2O_3}$ ($C_p$ in J/molK).

| | $Na_2O/(Al_2O_3 + Na_2O)$* | $a$ | $10^3 b$ |
|---|---|---|---|
| NATS 70:0 | 0.7014 | 132.3 | 25.7 |
| NATS 58:0 | 0.5869 | 93.7 | 56.4 |
| NATS 54:0 | 0.5515 | 81 | 72.9 |

* Values from Table 1.

Because we wish to interpret variations of our fit parameters in terms of physically meaningful features of melt structure, particular care has been taken to assess the uncertainties in calculated values of $S^{conf}$ $(T_g)$ and $B_e/S^{conf}(T_g)$. The need to consider all possible combinations of fit parameters which describe the data, rather than just the set of "best-fit" parameters has been recently illustrated by Russell et al., (2002). In order to quantify the confidence limits on each parameter, we have employed a bootstrap procedure to simulate sets of possible combinations of $A_e$, $B_e$ and $S^{conf}$ $(T_g)$ taking into account the uncertainty on individual measurements and the misfit of the data relative to the model. As a first step the best-fit parameters were determined by a least-squares regression of the viscosity data to a combination of equations 4 and 5. Secondly, the residuals for each data point were calculated and the magnitude of these residuals redistributed randomly among the data points and a new set of best-fit parameters calculated. This procedure was repeated 100 times for each composition, such that the 0.025 and 0.975 quantiles for each fit parameter (Table 5) and the correlations between fit parameters can be determined (Fig. 7). Qualitatively it may be noted that uncertainties on individual parameters are reduced when the liquid shows large departures from Arrhenian behaviour and/or when

Table 5. Coefficients of the Adam-Gibbs equation.

| | $T_{12}$ | $A_e$ | Q 0.025[a] | Q 0.975[a] | $10^{-5}$ $B_e$ | Q 0.025[a] | Q 0.975[a] | $S^{conf}$ ($T_g$) | Q 0.025[a] | Q 0.975[a] | $B_e/S^{conf}$ ($T_g$) |
|---|---|---|---|---|---|---|---|---|---|---|---|
| NATS 70:0 | 804 | −1.2 | −1.35 | −1.08 | 0.985 | 0.922 | 1.06 | 9.24 | 8.71 | 9.87 | 10660 |
| NATS 70:2 | 819 | −1.28 | −1.35 | −1.14 | 0.993 | 0.922 | 1.032 | 9.16 | 8.58 | 9.48 | 10840 |
| NATS 70:4 | 831 | −1.52 | −1.6 | −1.47 | 1.015 | 0.988 | 1.045 | 9.05 | 8.84 | 9.28 | 11215 |
| NATS 70:6 | 843 | −1.77 | −1.86 | −1.69 | 1.024 | 0.984 | 1.062 | 8.78 | 8.49 | 9.07 | 11663 |
| NATS 70:8 | 853 | | | | | | | | | | |
| NATS 70:10 | 863 | −1.56 | −1.62 | −1.5 | 0.961 | 0.931 | 0.991 | 8.2 | 7.97 | 8.43 | 11720 |
| NATS 58:0 | 887 | −1.1 | −1.48 | −0.79 | 1.21 | 1.02 | 1.44 | 10.35 | 8.98 | 12.12 | 11691 |
| NATS 58:4 | 907 | −1.58 | −1.85 | −1.31 | 1.16 | 1.014 | 1.319 | 9.47 | 8.39 | 10.55 | 12249 |
| NATS 58:8 | 906 | | | | | | | | | | |
| *NATS 58:10 | | | | | | | | | | | |
| NATS 54:0 | 939 | | | | | | | | | | |
| NATS 54:3 | 947 | | | | | | | | | | |
| *NATS 54:12 | 980 | | | | | | | | | | |
| NATS 50:0 | 1044 | | | | | | | | | | |
| NATS 50:2 | 1037 | | | | | | | | | | |
| *NATS 50:4 | 1047 | | | | | | | | | | |
| *NATS 50:6 | 1059 | | | | | | | | | | |
| *NATS 50:8 | 1057 | | | | | | | | | | |
| *NATS 50:10 | 1061 | | | | | | | | | | |

* Samples interpreted to be unmixed.

[a] Quantile 0.025 and Quantile 0.975. The real value of $S^{conf}$ ($T_g$) (which follow a non-gaussian distribution) has a probability of 0.95 of lying between these values.

the studied range of viscosity is large, particularly in the low temperature range.

When calculated values of configurational entropy are considered, it is found that addition of $TiO_2$ to NATS 70:00 decreases $S^{conf}$ at constant temperature (Fig. 8). Within the uncertainties associated with this approach, the decrease is linear with a value of approximately −2 J/mol.K at 900 K. Only two data points are available for the series NATS 58 and the error on $S^{conf}$ for these two compositions is too large to reach any meaningful conclusions. The results for the series NATS70 contrast with previous results in Al-free systems (Fig. 8), for which $S^{conf}$ was calculated to increase upon addition of $TiO_2$ (Bouhifd et al., 1999). Before considering the variation of the ratio $B_e/S^{conf}$ ($T_g$) upon addition of $TiO_2$ we underline the fact that this parameter has a much lower uncertainty than either $S^{conf}$ or $B_e$ when considered individually. This is because $S^{conf}$ and $B_e$ are highly correlated, as illustrated in Figure 7 for NATS 58:0. In this case, despite uncertainties in $B_e$ and $S^{conf}$ ($T_g$) of about 20%, the relative uncertainty in their ratio is only 2%. For the series NATS70 for which we have the most data, the variation of $B_e/S^{conf}$ ($T_g$) is clearly a non-linear function of $TiO_2$ with a sharp increase in $B_e/S^{conf}$ ($T_g$) for small additions of Ti followed by a plateau at additions greater than 6 mole% (Table 5). Further support for a non-linear variation is given by the non-linear dependence of melt fragility on $TiO_2$ content. This is because, given a linear variation of $C_p^{conf}$ and $S^{conf}$ ($T_g$) as a function of $TiO_2$, the only other parameter which can result in a non-linearity of fragility is $B_e/S^{conf}$ ($T_g$) (Toplis et al., 1997b). Interpretation of this result in terms of the structural role of Ti in our glasses will be discussed below.

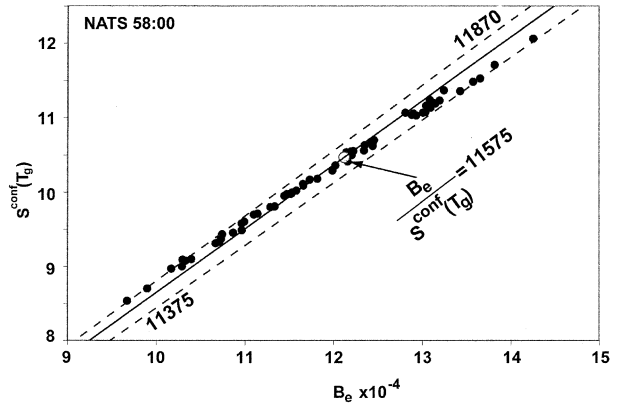


Fig. 7. Correlation between parameters $B_e$ and $S^{conf}$ ($T_g$) for the composition NATS 58:00. The open circle represents the best fit parameters. The solid lines represent the optimal value of the ratio $B_e/S^{conf}$ ($T_g$) and dashed lines, the extreme values for this ratio. Determination of this correlation is discussed in the text.

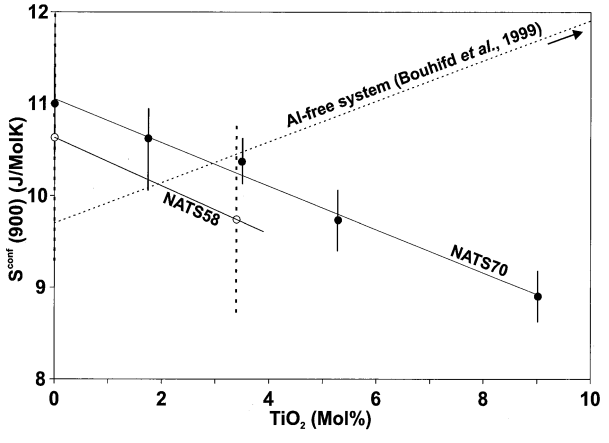


Fig. 8. Configurational entropy of melts at 900 K. Black circles = series NATS 70; open circles = series NATS 58; dashed line = extrapolation of the configurational entropy at 900K for NS2 and NTS2 melts as determined by Bouhifd et al. (1999). Determination of error bars as discussed in the text.

### 4.3. Implications for the Structural Role of Ti in Aluminosilicate Melts

The current view of the structural role of Ti in alkali silicate melts is that a dominant proportion of the Ti is present in a square pyramid geometry with one short titanyl (Ti=O) bond and four longer Ti–O bonds (Farges et al., 1996a, 1996b; Cormier et al., 1997, Reynard and Webb, 1998, Henderson et al., 2002). However, four or six fold coordinations are also inferred, with abundances on the order of a few tens of percent (Farges et al., 1996a; Farges, 1997). In the presence of aluminium, available spectroscopic evidence implies that five-fold coordinated Ti remains the dominant form (Farges et al., 1996a, Romano et al., 2000), although there is a trend to decreasing average coordination number as liquids become more polymerised (Farges and Brown, 1997). Below we will assess to what extent these conclusions are supported by our data and in addition we will address the question of whether there is any evidence for a specific interaction between Ti and Al in our glasses.

#### *4.3.1. Evidence for the coordination number of Ti*

One of the strongest constraints on the structural role of Ti in our glasses is given by the onset of anomalous behaviour and the saturation of anatase (Fig. 2). The fact that $TiO_2$ saturation is promoted by low $Na_2O$, high $Al_2O_3$ and high $TiO_2$ may be rationalized if a fraction of Ti requires the presence of Na in order to be stabilised, such that the solubility of Ti in the melt is limited by the availability of Na. This sort of behaviour has been previously described at superliquidus temperatures for potassium aluminosilicate melts by Dickinson and Hess (1985) and is to be expected if titanyl-bearing five-fold coordinated Ti is present because, using simple charge balance arguments, this structure requires an average of two Na atoms to be incorporated in the melt structure. Within the framework of this idea, the importance of aluminium may be understood because Al effectively locks Na in charge-balancing roles (Mysen, 1988) such that the latter are no longer available to stabilise Ti. If each Al is associated with one Na, and each Ti is associated with an average of $\varkappa$ Na the parameter Na*, defined as:

$$Na - Al - \varkappa.Ti, \tag{7}$$

is the number of 'free' Na remaining as network modifiers in the melt. Thus, one predicts that Na* falls to zero (accompanied by an onset of anomalous behaviour), upon addition of Ti to a base composition of fixed Na/(Na+Al) and that this transition from "normal" to "abnormal" behaviour will occur at lower Ti contents when Na/(Na+Al) is lower, in qualitative agreement with our observations (Fig. 2). In detail, the fact that composition NATS 54:6 shows abnormal behaviour while composition NATS 58:8 shows normal behaviour may be used to constrain the value of $\varkappa$. Assuming a common value of $\varkappa$ for both compositions and applying eq. 7, it is found that $\varkappa$ must be in the range 1.18 to 1.28, as illustrated in Figure 9. However, a potential complicating factor is that a proportion of Al may not be associated with Na in these compositions, for example due to the presence of triclusters containing one or more Al (Toplis et al., 1997a; Romano et al., 2000). In this case Na* as calculated using eqn. 7 will fall to zero even though some sodium

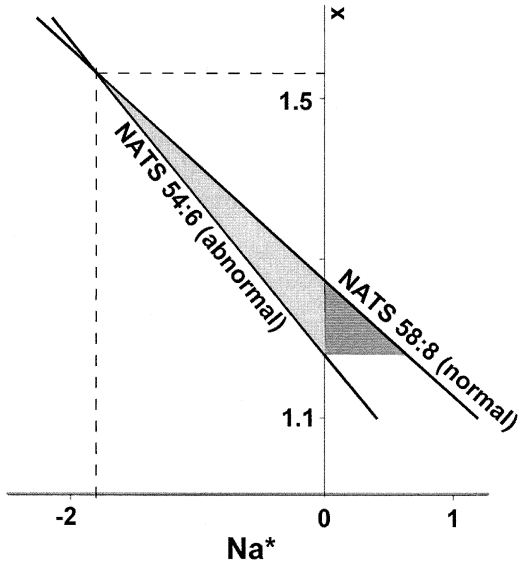


Fig. 9. Determination of the mean number of Na ($\varkappa$) associated with each Ti ($\varkappa$). The dark grey area represents the values of this parameter assuming the absence of Al-triclusters and the light grey area represents the range of number of Na per Ti if the formation of Al-triclusters is permitted. The dashed lines indicate the upper limits for the number of Al-bearing triclusters present in the melt and the average number of sodium per titanium atom (see text). Note that Figure 2 is an example of how the behaviour of samples varies as a function of Na* when $\varkappa$ is fixed to be 1.4.

remain in network modifying roles. The transition from normal to abnormal behaviour will therefore occur for negative values of Na*. For increasingly negative values of Na* at the transition from normal to abnormal behaviour, calculated values of $\varkappa$ increase (Fig. 9). However the range of values decreases and an absolute upper limit to $\varkappa$ of 1.54 is determined because for higher values of $\varkappa$, composition NATS 58:8 has a lower calculated Na* than composition NATS 54:6 even though the former shows normal behaviour and the latter abnormal behaviour. This reasoning also places an upper limit of no more than 6 relative percent of Al not associated with charge-balancing sodium. We also note that although $\varkappa$ is not necessarily identical for compositions NATS 54:6 and NATS 58:8, there is no reason to expect variations in this parameter to be outside the range calculated above.

The value of $\varkappa$ is a function of the nature and the relative proportions of the structural environment(s) of Ti. If one assumes that Ti in our samples is a mixture of five-fold coordinated titanyl-bearing moities and one or more additional environments which do not require any Na (four and/or six-fold coordination), our calculated range of $\varkappa$ implies a dominant proportion of the titanyl groups (60–75%), relative species proportions in excellent agreement with values determined spectroscopically (Farges et al., 1996a). On the other hand we cannot exclude the possibility that another mechanism involving only one Na to stabilise one Ti may be operating, in which case the real proportion of titanyl bearing $^{[V]}Ti$ will be lower than calculated above. Furthermore, we note that our estimated values of $\varkappa$ are only valid for samples annealed near the glass transition and that the average number of Na associated with Ti may be a function of temperature. For example, Dickinson and

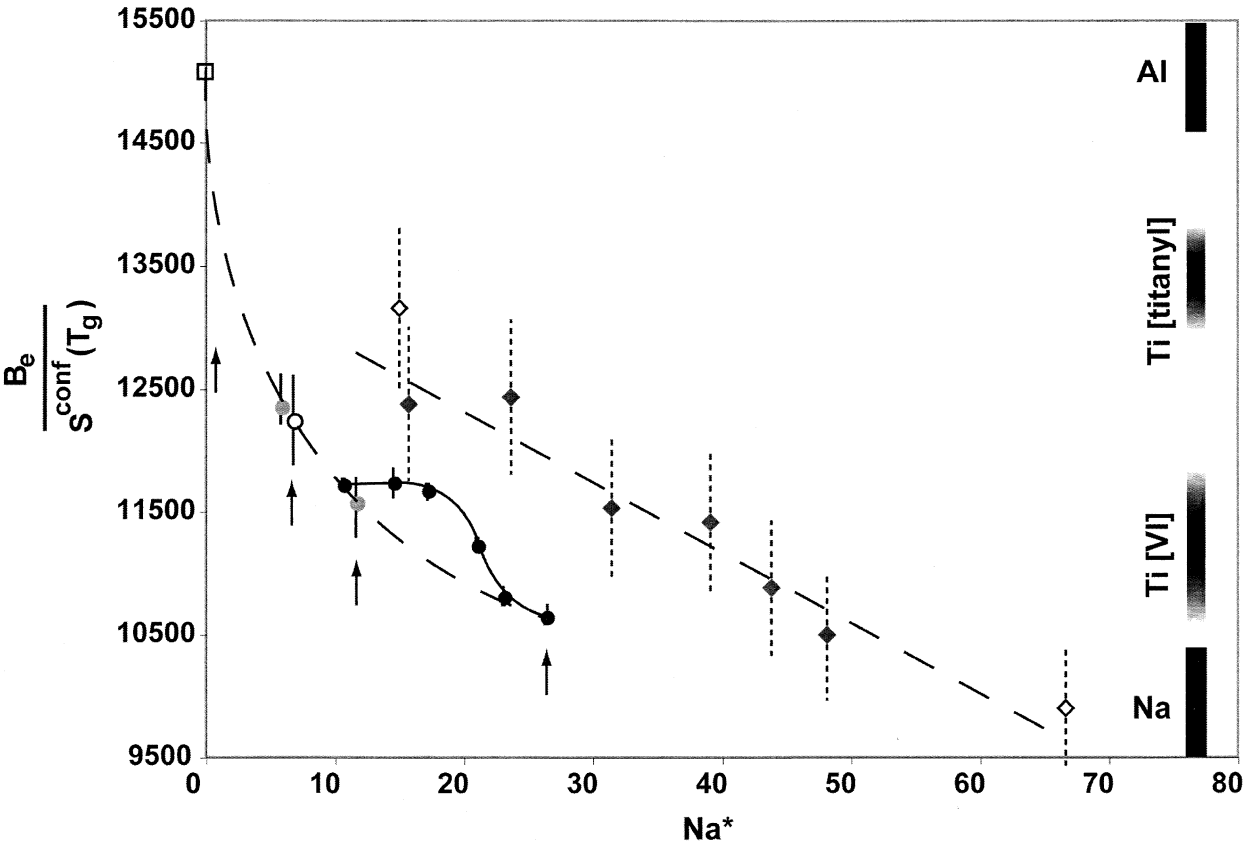


Fig. 10. Variation of $B_e/S^{conf}$ ($T_g$) as a function of Na*, the latter calculated assuming 1.4 Na per Ti. Diamonds are data from Bouhifd et al. (1999) and Liska et al. (1996) for sodium titanosilicate melts (Open and filled respectively). In the absence of a detailed statistical study, error bars have been set to 5 relative%. The dashed line is a linear fit to the data, clearly showing the increase in $B_e/S^{conf}$ ($T_g$) upon addition of titania. The open square is the value of $B_e/S^{conf}$ ($T_g$) for jadeite melt taken from Toplis (1998). Data from this study are represented by circles (black circles = NATS 70, grey circles = NATS 58 and open circle = NATS 54:00. The dashed curve links the Ti-free compositions used in this study (indicated by arrows). Bars shown on the right hand side of the diagram represent semiquantitative estimates of the range of $B_e/S^{conf}$ ($T_g$) associated with different individual microscopic mechanisms controlling viscous flow (see text for more details).

Hess inferred an average K/Ti of only approximately 0.7 in the superliquidus range although to what extent this is due to the difference in the nature of the metal cation (Na *vs.* K) cannot be directly assessed. However, we note that the fact that significant amounts of Ti may be incorporated in metaluminous and even peraluminous melts in the superliquidus range (Dickinson and Hess, 1985) despite the fact that those compositions contain no nominal 'free' alkalis, provides indirect evidence in favour of a reduction of $\varkappa$ with increasing temperature.

Further indirect evidence for the coordination state of Ti in our glasses is provided by consideration of the ratio $B_e/S^{conf}$ ($T_g$) and its variation as a function of $TiO_2$. If it is accepted that $B_e/S^{conf}$ ($T_g$) is directly proportional to the average energy barrier to viscous flow (Toplis, 1998), interpretation of this parameter requires consideration of the potential microscopic mechanisms of viscous flow which may be operating. For example, in Ti-free peralkaline melts, viscous flow is thought to involve production and elimination of five-coordinated network formers, formed through interaction with non-bridging oxygens (NBO) (e.g. Stebbins, 1991). When no NBO are available (for example in metaluminous compositions or $SiO_2$) other mechanisms must be active and energy barriers to viscous flow are expected to be higher than in peralkaline melts. In Na-bearing systems it may be noted that this energy barrier shows smooth, albeit non-linear, variations going from compositional fields where a mechanism involving $NBO_{Na}$ dominates to those where an alternative mechanism dominates (Toplis, 1998). In light of the potential importance of $NBO_{Na}$, values of $B_e/S^{conf}$ ($T_g$) have been considered as a function of Na* (Fig. 10). When considered in this way, literature data for Al-free systems (Liska et al., 1996; Bouhifd et al., 1999) show that $B_e/S^{conf}$ ($T_g$) increases in a linear fashion with decreasing Na*. This observation cannot be simply explained in terms of removal of $NBO_{Na}$ which would result in a highly non-linear variation of $B_e/S^{conf}$ ($T_g$) (Toplis, 1998). Rather, it infers that the average energy barrier is increasingly dominated by the contribution of a mechanism involving titanium. Given that five-fold coordinated titanyl is the dominant form of Ti in sodium silicate melts (Farges et al., 1996a), we assume that this is the species that takes part in the viscous flow mechanism. In light of this observation it is of interest to note that, for additions of up to 6% $TiO_2$ to NATS70, $B_e/S^{conf}$ ($T_g$) tends towards the same endmember value of 13500. However, for greater additions of $TiO_2$ this trend is interrupted and reaches an apparent plateau.

Interpretation of this feature is necessarily qualitative, but is consistent with the emergence of an additional viscous flow mechanism with an energy barrier significantly lower than that attributed to $^{[V]}Ti$. Network forming $^{[IV]}Ti$ may be expected to have a high energy barrier to viscous flow (not as high as that operating in $SiO_2$, but higher than that in depolymerised compositions), thus we feel that the simplest explanation would be an increasing role of octahedral $^{[VI]}Ti$ which forms $NBO_{Ti}$. The increasing role of this 'low energy barrier' mechanism (whatever its structural origin) may imply changes in the relative proportions of $^{[n]}Ti$ as a function of $TiO_2$ content (e.g. Henderson and Fleet, 1995; Mysen and Neuville, 1995), but this is not necessarily the case. This observation could also be explained by increasing connectivity of regions of the melt structure in which the non-titanyl coordination state is concentrated. For example, in the case that non-titanyl Ti is $^{[VI]}Ti$ this would result in a model of melt structure resembling that of the modified random network model in which network modifier-rich regions are envisaged as channels through the melt structure. This result leads us to consider the longer range order of Ti in our glasses and the question of a possible Al-Ti interaction.

#### *4.3.2. Evidence for next-nearest-neighbour interactions*

One of the most striking results of this study is that configurational entropy decreases as titanium is added (Fig. 8). This is indeed a surprising result because addition of extra components almost always increases configurational entropy. It also contrasts with the case of addition of $TiO_2$ to Al-free compositions, for which $S^{conf}$ increases (Bouhifd et al., 1999, and Fig. 8). The likely explanation of this result is that Ti imposes a strong degree of structural order amongst its next-nearest-neighbours. Several options are possible, such as only Si as adjacent network forming cations to the four oxygens at the base of the titanyl-bearing $^{[V]}Ti$, or only Al, or some fixed ratio of Al and Si. Another possibility, consistent with the recent proposal of Romano et al. (2000) is that Ti is pushing Al and Si into highly ordered configurations such as triclusters of some fixed Si/Al ratio. This latter possibility also has the consequence that it liberates Na from charge balancing roles which may then stabilise further titanyl-bearing Ti in the melt. However, we do not favour this hypothesis for our glasses in the studied temperature range because as discussed above, the saturation of $TiO_2$ in our liquids (Fig. 9) would imply that no more than 6 relative percent of Al occur in triclusters. Further indirect evidence that the structural role of Al is not significantly modified upon addition of $TiO_2$ is the fact that single values for $\bar{C}_{p\ Al_2O_3}$ and $\bar{C}_{pTiO_2}$ can account for all heat capacity data of each series of constant Na/(Na + Al). Indeed, the lack of any excess $C_p$ terms provides evidence against a strong interaction of $TiO_2$ with $Al_2O_3$. Furthermore, the fact that the unusual temperature dependence of $C_p$ in titanium-bearing melts can be predicted, within experimental errors, from the partial molar $C_p$ for $TiO_2$ determined in Al-free melts, suggests to us that the local structural environment of Ti is identical in both Al-free and Al-bearing melts (*i.e.* Ti–O are surrounded only by Si). This leads us to propose that our melts are composed of two more or less connected sub-domains; one in which titanium and $SiO_2$ tetrahedra are concentrated, the other in which tetrahedral alumina charge balanced by sodium and $SiO_2$ are concentrated. This model is similar in many ways to that of Farges et al. (1996b) although the latter is for Al-free systems. In our model, the local environments of Al and Ti are unrelated and the poor mixing of the structural units as well as the progressive removal of sodium from network-modifying roles as titanium is added to the melt would both act to decrease the configurational entropy. However, we stress again that these implications may only be valid at temperatures close to the glass transition and that the same melts at superliquidus conditions may be structurally different. We do not exclude that at higher temperature, increasing disorder of Al and Si may occur around Ti atoms, or even that triclusters may be present and possibly frozen in during rapid quenching to glass, thus explaining the results of Romano et al. (2000). Indeed, it is of note that incomplete mixing of titanium with $SiO_4^{4-}$ tetrahedra around $T_g$ has been previously proposed on thermodynamic and structural grounds for titanosilicate melts (Gan et al., 1996; Henderson and Fleet, 1997; Bouhifd et al., 1999; Krocker et al., 2002) in support of this contention.

## 5. CONCLUDING REMARKS

As discussed above, our measurements of heat capacity and shear viscosity may be used, either individually or in combination, to provide insights into the structural role of Ti in aluminosilicate glasses and liquids. The conclusions concerning the immediate coordination environment of Ti are in broad agreement with previous studies, although new spectroscopic data are clearly needed to determine the exact nature of non-titanyl Ti in these compositions. Furthermore, the lack of evidence of an interaction between Ti and Al as well as the fact that configurational entropy decreases upon addition of Ti, both point to an important role of medium range order in controlling the macroscopic properties of these liquids. Changes in medium range order may occur, not only in response to changes in glass composition, but also as a function of temperature for a single glass composition, thus, further constraints on the temperature and compositional dependence of medium range aspects of melt structure are required in order to fully understand the relationships between structure and properties of titanium-bearing melts.

*Acknowledgments*—We thank N. Dauphas for help in calculating uncertainties when fitting viscosity data, P. Jarry and Y. Linard for their help with calorimetric measurements, B. Reynard and the Raman spectroscopy facility at the LST (Lyon) for the characterization of partially crystallized samples, and P. Besson for help with the TEM. Numerous fruitful discussions with A. Bouhifd are much appreciated. G. S. Henderson and three anonymous reviewers are thanked for helpful comments, as well as J. K. Russell for editorial handling. This work is CRPG contribution number 1642.

*Associate editor:* K. J. Russell

## REFERENCES

Adam G. and Gibbs J. H. (1965) On the temperature dependence of cooperative relaxation properties in glass-forming liquids. *J. Chem. Phys.* **43,** 139–146.

Angell C. A. (1985) Strong and fragile liquids. In *Relaxations in complex systems* (eds. K. L. Ngai and G. B. Wright), pp. 3–11. U. S. Departement of Commerce National Technical Information Service, Springfield, Virginia.

Angell C. A. (2001) A thermodynamic connection to the fragility of glassforming liquids. *Nature* **410,** 663–666.

Bottinga Y. and Weill D. F. (1970) Densities of liquid silicate systems calculated from partial molar volumes of oxide components. *Am. Jour. Sci.* **269,** 169–182.

Bouhifd M. A., Sipp A., and Richet P. (1999) Heat capacity, viscosity, and configurational entropy of alkali titanosilicate melts. *Geochim. Cosmochim. Acta* **63,** 2429–2438.

Courtial P. and Richet P. (1993) Heat capacity of magnesium aluminosilicate melts. *Geochim. Cosmochim. Acta* **57,** 1267–1275.

Dickinson J. E. and Hess P. C. (1985) Rutile solubility and titanium coordination in silicate melts. *Geochim. Cosmochim. Acta* **49,** 2289–2296.

Dingwell D. B. (1992 a) Density of some titanium-bearing silicate liquids and the compositional dependence of the partial molar volume of $TiO_2$. *Geochim. Cosmochim. Acta* **56,** 3403–3407.

Dingwell D. B. (1992 b) Shear viscosity of alkali and alkaline earth titanium silicate liquids. *Amer. Mineral.* **77,** 270–274.

Farges F. (1997) Coordination of $Ti^{4+}$ in silicate glasses: A high-resolution XANES spectroscopy study at the Ti *K* edge. *Am. Min.* **82,** 36–43.

Farges F., Brown G. E. Jr., Navrotsky A., Gan H., and Rchr J. J. (1996a) Coordination chemistry of Ti (IV) in silicate glasses and melts: II. Glasses at ambient temperature and pressure. *Geochim. Cosmochim. Acta* **60,** 3039–3053.

Farges F., Brown G. E. Jr., Navrotsky A., Gan H., and Rehr J. J. (1996b) Coordination chemistry of Ti (IV) in silicate glasses and melts: III. Glasses and melts from ambient to high temperature. *Geochim. Cosmochim. Acta* **60,** 3055–3065.

Farges F. and Brown G. E. Jr. (1997) Coordination chemistry of Ti (IV) in silicate glasses and melts: IV. XANES studies of synthetic and natural volcanic glasses and tektites at ambient temperature and pressure. *Geochim. Cosmochim. Acta* **61,** 1863–1870.

Gan H., Wilding M. C., and Navrotsky A. (1996) $Ti^{4+}$ in silicate melts: Energetics from high-temperature calorimetric studies and implications for melt structure. *Geochim. Cosmochim. Acta* **60,** 4123–4131.

Glasser F. P. and Maar J. (1979) Phase relations in the system $Na_2O$-$TiO_2$-$SiO_2$. *J. Amer. Ceram. Soc.* **62,** 42–47.

Haggerty J. S., Cooper A. R., and Heasley J. H. (1968) Heat capacity of three inorganic glassesand supercooled liquids. *Phys. Chem. Glasses* **5,** 130–136.

Henderson G. S. and Fleet M. E. (1995) The structure of Ti silicate glasses by micro-Raman spectroscopy. *Can. Mineral.* **33,** 399–408.

Henderson G. S. and Fleet M. E. (1997) The structure of titanium glasses investigated by K-edge X-ray absorption spectroscopy. *J. Non-cryst. Solids* **211,** 214–221.

Henderson G. S., Liu X., and Fleet M. E. (2002) A Ti-L-edge X-ray absorption study of Ti-silicate glasses. *Phys. Chem. Min* **29,** 32–42.

Jarry P. and Richet P. (2001) Unmixing in sodium-silicate melts: influence on viscosity and heat capacity. *J. Non-Cryst. Solids* **293/295,** 232–237.

Krocker S., Rice D., and Stebbins J. F. (2002) Disordering during melting: an oxygen-17 NMR study of crystalline and glassy $CaTiSiO_5$ (titanite). *Amer. Miner.* **87,** 572–579.

Lange R. A. and Carmichael I. S. E. (1987) Densities of $Na_2O$-$K_2O$-CaO-MgO-FeO-$Fe_2O_3$-$Al_2O_3$-$TiO_2$-$SiO_2$ liquids : new measurements and derived partial molar properties. *Geochim. Cosmochim. Acta* **51,** 2931–2946.

Lange R. A. and Navrotsky A. (1992) Heat capacities of $Fe_2O_3$-bearing silicate liquids. *Contrib. Mineral. Petrol* **110,** 311–320.

Lange R. A. and Navrotsky A. (1993) Heat capacities of $TiO_2$-bearing silicate liquids: Evidence for anomalous change in configurational entropy with temperature. *Geochim. Cosmochim. Acta* **57,** 3001–3011.

Lejeune A. M. and Richet P. (1995) Rbeology of crystal-bearing silicate melts: an experimental study at high viscosities. *J. Geophys. Res.* **100,** 4215–4229.

Linard Y., Yamashita I., Atake T., Rogez J., and Richet P. (2001) Thermochemistry of nuclear waste glasses : an experimental determination. *J. Non-Cryst. solids* **286,** 200–209.

Liska M., Simurka P., Antalik J., and Perichta P. (1996) Viscosity of titania-bearing sodium silicate melts. *Chem. Geol* **128,** 199–206.

Liu Q. and Lange R. A. (2001) The partial molar volume and thermal expansivity of $TiO_2$, in alkali silicate melts: Systematic variation with Ti coordination. *Geochim. Cosmochim. Acta* **65,** 2379–2393.

Longhi J. (1992) Experimental petrology and petrogenesis of mare volcanics. *Geochim. Cosmochim. Acta* **56,** 2235–2251.

Mysen B. O. (1988) *Structure and properties of silicate melts*. Elsevier, Amsterdam. p. 354.

Mysen B. O. and Neuville D. R. (1995) Effect of temperature and $TiO_2$ content on the structure of $Na_2Si_2O_5$-$Na_2Ti_2O_5$ melts and glasses. *Geochim. Cosmochim. Acta* **59,** 325–342.

Neuville D. R. and Richet P. (1991) Viscosity and mixing in molten (Ca, Mg) pyroxenes and garnets. *Geochim. Cosmochim. Acta* **55,** 1011–1019.

Reynard B. and Webb S. L. (1998) High-temperature Raman spectroscopy of $Na_2TiSi_2O_7$ glass and melt: coordination of $Ti^{4+}$ and the nature of the configurational changes in the liquid. *Eur. J. Mineral.* **10,** 49–58.

Richet P. (1984) Viscosity and configurational entropy of silicate melts. *Geochim. Cosmochim. Acta* **48,** 471–483.

Richet P. (1987) Heat capacity of silicate glasses. *Chem. Geol.* **62,** 111–124.

Richet P. and Bottinga Y. (1984) Glass transition and thermodynamic properties of amorphous $SiO_2$, $NaAlSi_nO_{2n+2}$ and $KAlSi_3O_8$. *Geochim. Cosmochim. Acta* **48,** 453–470.

Richet P. and Bottinga Y. (1985) Heat capacity of aluminum-free liquid silicates. *Geochim. Cosmochim. Acta* **49,** 471–486.

Richet P. and Bottinga Y. (1986) Thermochemical properties of silicate glasses and liquids: a review. *Rev. Geophys* **24,** 1–25.

Richet P. and Neuville D. R. (1992) Thermodynamics of silicate melts: Configurational properties. In *Adv Phys Geochem* vol. 11 (ed. S. Saxena), Springer-Verlag, Heidelberg. pp. 132–160.

Romano C., Paris E., Poe B. T., Giuli G., Dingwell D. B., and Mottana A. (2000) Effect of aluminum on Ti-coordination in silicate glasses: A XANES study. *Amer. Mineral.* **85,** 108–117.

Russell J. K., Giordano D., Dingwell D. B., and Hess K.-U. (2002) Modelling the non-Arrhenian rheology of silicate melts: Numerical considerations. *Eur. J. Mineral.* **14-2,** 417–428.

Simmons J. H., Mills S. A., and Napolitano A. (1974) Viscous flow in glass during phase separation. *J. Amer. Ceram. Soc.* **57,** 109–116.

Sipp A., Neuville D. R., and Richet P. (1997) Viscosity, configurational entropy and relaxation kinetics of borosilicate melts. *J. Non-Cryst. Solids* **211,** 281–293.

Sipp, A. (1998) Propriétés de relaxation des silicates vitrcux et fondus. *Thesis*, University Paris VII, pp 231.

Sipp A. and Richet P. (2002) Equivalence of the kinetics of volume, enthalpy and viscosity relaxation in glass-forming silicate liquids. *J. Non-Cryst. Solids* **298,** 202–212.

Stebbins J. F. (1991) Experimental confirmation of five-coordinated silicon in a silicate glass at 1 atmosphere pressure. *Nature* **351,** 638–639.

Stebbins J. F., Carmichael I. S. E., and Weill D. E. (1983) The high temperature liquid and glass heat contents and the heats of fusion of diopside, albite, sanidine and nepheline. *Amer. Mineral* **68,** 717–730.

Stebbins J. F., Carmichael I. S. E., and Moret L. K. (1984) Heat capacities and entropies of silicate liquids and glasses. *Contrib. Mineral. Petrol* **86,** 371–385.

Tangeman J. A. and Lange R. A. (1998) The effect of $Al^{3+}$, $Fe^{3+}$, and $Ti^{4+}$ on the configurational heat capacities of sodium silicate liquids. *Phys. Chem. Minerals* **26,** 83–99.

Toplis M. J. (1998) Energy barriers to viscous flow and the prediction of glass transition temperature of molten silicates. *Amer. Mineral.* **83,** 480–490.

Toplis M. J. and Dingwell D. B. (1995) The influence of $TiO_2$ on viscosities of melts of variable alkali/aluminium ratio. *EOS* **76,** 649.

Toplis M. J., Dingwell D. B., and Lenci T. (1997a) Peraluminous viscosity maxima in $Na_2O$-$Al_2O_3$-$SiO_2$ liquids: The role of triclusters in tectosilicate melts. *Geochim. Cosmochim. Acta* **61,** 2605–2612.

Toplis M. J., Dingwell D. B., Hess K., and Lenci T. (1997b) Viscosity, fragility, and configurational entropy of melts along the join $SiO_2$-$NaAlSiO_4$. *Amer. Mineral.* **82,** 979–990.

Toplis M. J., Gottsmann J., Knoche R., and Dingwell D. B. (2001) Heat capacities of haplogranitic glasses and liquids. *Geochim. Cosmochim. Acta* **65,** 1985–1994..

Appendix 1. Heat capacity data (NATS 70)

| T (K) | NATS 70:0 | T (K) | NATS 70:2 | T (K) | NATS 70:4 | T (K) | NATS 70:6 | T (K) | NATS 70:10 |
|---|---|---|---|---|---|---|---|---|---|
| 316.85 | 56.327 | 305.20699 | 54.16861757 | 305.16337 | 53.48926366 | 316.86 | 55.183 | 316.86 | 55.634 |
| 341.87 | 58.45 | 315.21743 | 58.07022829 | 315.22061 | 55.5676099 | 341.87 | 57.7 | 341.86 | 58.081 |
| 366.74 | 60.6 | 325.16192 | 58.82223647 | 325.16416 | 56.7447635 | 366.73 | 59.803 | 366.72 | 60.191 |
| 391.6 | 62.311 | 335.10639 | 57.96697327 | 335.10845 | 57.17035737 | 391.59 | 61.464 | 391.58 | 61.916 |
| 415.46 | 63.57 | 345.05168 | 58.7780771 | 345.05321 | 57.87294573 | 416.45 | 62.843 | 416.44 | 63.277 |
| 441.32 | 65.131 | 354.99608 | 59.87491806 | 354.99762 | 59.19730522 | 441.3 | 64.442 | 441.3 | 64.857 |
| 466.17 | 66.333 | 364.93929 | 60.07688226 | 364.94157 | 59.86469899 | 466.15 | 65.698 | 466.15 | 66.109 |
| 491.03 | 67.658 | 374.8836 | 60.61978282 | 374.88605 | 60.47343509 | 491.01 | 66.961 | 491.01 | 67.423 |
| 515.89 | 68.666 | 384.82787 | 61.40620935 | 384.83149 | 60.92184028 | 515.86 | 68.27 | 515.86 | 68.4 |
| 540.75 | 69.952 | 394.77186 | 61.89910591 | 394.77512 | 61.60357257 | 540.72 | 69.213 | 540.71 | 69.469 |
| 565.61 | 70.85 | 404.71502 | 62.73748464 | 404.71856 | 62.07283381 | 565.57 | 69.907 | 565.57 | 70.262 |
| 590.46 | 71.878 | 414.65784 | 63.17128557 | 414.66305 | 62.66853488 | 590.43 | 70.816 | 590.42 | 71.397 |
| 615.32 | 72.55 | 424.60035 | 63.59664426 | 424.60622 | 63.36395397 | 615.28 | 71.85 | 615.28 | 72.169 |
| 640.17 | 73.597 | 434.54383 | 64.0356404 | 434.54931 | 63.84755375 | 640.13 | 72.531 | 640.13 | 73.074 |
| 665.02 | 74.301 | 444.48514 | 64.68699119 | 444.49253 | 64.48105642 | 664.98 | 73.284 | 664.98 | 73.879 |
| 689.88 | 75.07 | 454.42972 | 65.20131804 | 454.43587 | 65.05068742 | 689.83 | 74.03 | 689.83 | 74.619 |
| 714.72 | 75.742 | 464.37171 | 65.98774456 | 464.37841 | 65.49453034 | 714.67 | 74.547 | 714.68 | 75.167 |
| 739.59 | 76.537 | 474.31457 | 66.1221709 | 474.32064 | 66.01202121 | 739.52 | 75.228 | 739.53 | 75.734 |
| 764.45 | 77.862 | 484.2571 | 67.02613929 | 484.26314 | 66.5575374 | 764.4 | 76.17 | 764.41 | 76.705 |
| 789.31 | 79.775 | 494.19872 | 67.5320239 | 494.20495 | 66.98573828 | 789.26 | 77.014 | 789.27 | 77.523 |
| 814.16 | 88.59 | 504.14063 | 68.15739859 | 504.14652 | 67.51496067 | 814.11 | 78.566 | 814.12 | 78.672 |
| 839.02 | 91.466 | 514.08288 | 68.26195241 | 514.0884 | 68.0344068 | 838.96 | 83.317 | 838.97 | 80.633 |
| 863.87 | 92.959 | 524.02607 | 68.69380512 | 524.02962 | 68.3772282 | 863.81 | 95.661 | 863.82 | 92.833 |
| 888.71 | 93.146 | 533.96772 | 69.26787701 | 533.9701 | 69.2681728 | 888.66 | 96.911 | 888.67 | 99.045 |
| 913.56 | 93.062 | 543.91102 | 69.55880936 | 543.91135 | 69.28381484 | 913.5 | 96.852 | 913.51 | 101.74 |
| 938.41 | 92.939 | 553.85282 | 69.75882536 | 553.85145 | 69.73743404 | 938.35 | 96.459 | 938.35 | 101.26 |
| 963.25 | 93.062 | 563.79447 | 70.774491 | 563.79355 | 70.10502201 | 963.19 | 96.302 | 963.2 | 101.01 |
| 988.09 | 93.191 | 573.73716 | 70.74851489 | 573.73493 | 70.35855343 | 988.02 | 96.014 | 988.04 | 100.61 |
| 1012.9 | 93.237 | 583.67686 | 71.3024553 | 583.6746 | 70.72418614 | 1012.9 | 95.844 | 1012.9 | 100.11 |
| 1037.8 | 93.437 | 593.61741 | 71.4037621 | 593.61472 | 71.0663558 | 1037.7 | 95.517 | 1037.7 | 99.903 |
| 1062.6 | 93.526 | 603.55631 | 71.49143145 | 603.5546 | 71.36430633 | 1062.5 | 95.393 | 1062.5 | 99.883 |
| | | 613.49671 | 72.0577105 | 613.49613 | 71.72853554 | | | | |
| | | 623.43409 | 72.57333615 | 623.43714 | 72.19649328 | | | | |
| | | 633.37305 | 72.75322066 | 633.37427 | 72.55495673 | | | | |
| | | 643.31083 | 73.0629857 | 643.31562 | 72.82738894 | | | | |
| | | 653.25272 | 73.4415874 | 653.25544 | 73.25558982 | | | | |
| | | 663.1948 | 73.60393805 | 663.19321 | 73.47848891 | | | | |
| | | 673.13456 | 73.78901778 | 673.1301 | 73.78937448 | | | | |
| | | 683.07307 | 74.044233 | 683.07114 | 73.9484019 | | | | |
| | | 693.01026 | 74.3455558 | 693.00898 | 74.28340229 | | | | |
| | | 702.94941 | 74.63453994 | 702.94587 | 74.39550358 | | | | |
| | | 712.88416 | 74.98391853 | 712.88184 | 74.7448425 | | | | |
| | | 722.82139 | 75.38719754 | 722.82105 | 74.97425911 | | | | |
| | | 732.76032 | 75.36511785 | 732.75916 | 75.41875378 | | | | |
| | | 742.69874 | 75.78852833 | 742.6951 | 75.83913364 | | | | |
| | | 752.63715 | 75.98529731 | 752.63282 | 76.43678997 | | | | |
| | | 762.57465 | 76.86978363 | 762.57133 | 76.60689717 | | | | |
| | | 772.51349 | 77.013951 | 772.50855 | 77.04226732 | | | | |
| | | 782.45023 | 77.75232174 | 782.44422 | 77.40138252 | | | | |
| | | 792.38596 | 78.34132988 | 792.38145 | 78.12873744 | | | | |
| | | 802.32322 | 78.53290364 | 802.31571 | 78.78896193 | | | | |
| | | 812.26041 | 80.41617113 | 812.25413 | 79.69620032 | | | | |
| | | 822.19712 | 82.92091689 | 822.19089 | 81.90107639 | | | | |
| | | 832.13407 | 87.7784482 | 832.12559 | 86.64387366 | | | | |
| | | 842.07505 | 90.75660844 | 842.06449 | 91.03342149 | | | | |
| | | 852.01517 | 93.03601151 | 851.99967 | 93.82813287 | | | | |
| | | 861.95334 | 93.65229456 | 861.93522 | 94.03089678 | | | | |
| | | 871.892 | 93.82958146 | 871.87266 | 95.78273627 | | | | |
| | | 881.8259 | 93.74321092 | 881.81565 | 95.44838764 | | | | |
| | | 891.76383 | 94.08414727 | 891.75339 | 95.71886461 | | | | |
| | | 901.69535 | 94.18675288 | 901.69016 | 95.32194781 | | | | |
| | | 911.62888 | 94.76212357 | 911.62131 | 95.4529499 | | | | |
| | | 921.56449 | 94.10427876 | 921.55759 | 95.82053787 | | | | |
| | | 931.50217 | 92.80287598 | 931.49412 | 95.69540154 | | | | |
| | | 941.43882 | 93.93218707 | 941.43235 | 95.35649065 | | | | |
| | | 951.37321 | 93.94712333 | 951.3657 | 95.19550797 | | | | |
| | | 961.3082 | 93.61008339 | 961.2999 | 95.4125413 | | | | |
| | | 971.24216 | 94.38222306 | 971.2335 | 95.11403901 | | | | |

(Continued)

Appendix 1. Heat capacity data (NATS 70) (Continued)

| T (K) | NATS 70:0 | T (K) | NATS 70:2 | T (K) | NATS 70:4 | T (K) | NATS 70:6 | T (K) | NATS 70:10 |
|---|---|---|---|---|---|---|---|---|---|
| | | 981.17411 | 94.28805969 | 981.16733 | 95.03061479 | | | | |
| | | 991.10496 | 94.55301594 | 991.09849 | 95.30826102 | | | | |
| | | 1001.03892 | 94.57574503 | 1001.03141 | 95.43600436 | | | | |
| | | 1010.97111 | 94.32962145 | 1010.96293 | 95.47315421 | | | | |
| | | 1020.90336 | 95.0212352 | 1020.89176 | 95.23917534 | | | | |
| | | 1030.83188 | 94.26208358 | 1030.82017 | 95.76122847 | | | | |
| | | 1040.76041 | 94.61470918 | 1040.74924 | 95.25481738 | | | | |
| | | 1050.68961 | 95.61673737 | 1050.67808 | 95.83161765 | | | | |
| | | 1060.6179 | 94.43352586 | 1060.60416 | 95.23722009 | | | | |
| | | 1070.54661 | 93.98219107 | 1070.53354 | 95.57678273 | | | | |
| | | 1080.47379 | 95.2296343 | 1080.4592 | 94.92959327 | | | | |
| | | 1090.40128 | 94.09583652 | 1090.38901 | 96.13859271 | | | | |

Appendix 1. Heat capacity data (NATS 58)

| T (K) | NATS 58:0 | T (K) | NATS 58:4 | T (K) | NATS 58:8 | T (K) | NATS 58:10 | T (K) | NATS 58:11 |
|---|---|---|---|---|---|---|---|---|---|
| 311.9287 | 56.14992 | 305.4263 | 57.10259 | 305.3394 | 55.64136 | 305.1503 | 56.11871 | 305.1529 | 56.0561 |
| 336.9412 | 58.61364 | 315.4427 | 57.96069 | 315.3538 | 57.52086 | 315.1566 | 57.02315 | 315.1625 | 57.59123 |
| 361.803 | 61.02235 | 325.3883 | 58.57524 | 325.2987 | 58.13213 | 325.1012 | 58.56185 | 325.1071 | 58.48215 |
| 386.6582 | 62.88555 | 335.3333 | 60.16467 | 335.243 | 58.96306 | 335.0453 | 58.74626 | 335.0517 | 59.18651 |
| 411.5096 | 64.5446 | 345.2781 | 59.80968 | 345.1875 | 59.67913 | 344.9904 | 59.5048 | 344.9957 | 59.90845 |
| 436.3645 | 66.1387 | 355.2247 | 60.28611 | 355.1314 | 60.44154 | 354.9349 | 60.135 | 354.9404 | 60.77707 |
| 461.2175 | 67.64729 | 365.1713 | 61.74475 | 365.0759 | 61.08841 | 364.8779 | 60.85235 | 364.8846 | 61.41586 |
| 486.0706 | 68.98885 | 375.1169 | 61.57327 | 375.0207 | 61.72253 | 374.822 | 61.54402 | 374.8293 | 61.99246 |
| 510.9067 | 70.23695 | 385.0611 | 63.0179 | 384.9664 | 62.33044 | 384.7655 | 62.22961 | 384.7741 | 62.60827 |
| 535.7571 | 71.39159 | 395.0067 | 63.40158 | 394.9102 | 62.92761 | 394.7089 | 62.84766 | 394.7172 | 63.29032 |
| 560.6111 | 72.46735 | 404.9518 | 63.9821 | 404.8543 | 63.61277 | 404.6529 | 63.39546 | 404.6606 | 63.86557 |
| 585.4622 | 73.449 | 414.899 | 64.70274 | 414.7994 | 64.28047 | 414.5962 | 64.12833 | 414.6039 | 64.526 |
| 610.3149 | 74.43064 | 424.842 | 65.14648 | 424.7435 | 64.85346 | 424.539 | 64.73895 | 424.5475 | 65.08908 |
| 635.1689 | 75.15577 | 434.7888 | 65.86378 | 434.6877 | 65.3727 | 434.481 | 65.41306 | 434.4899 | 65.63526 |
| 660.023 | 76.08903 | 444.7313 | 66.46899 | 444.6303 | 65.99002 | 444.4229 | 66.07569 | 444.4336 | 66.21457 |
| 684.8673 | 76.78301 | 454.6805 | 66.87003 | 454.5746 | 66.45687 | 454.3657 | 66.40261 | 454.3757 | 66.76886 |
| 709.6804 | 77.46771 | 464.6227 | 67.56398 | 464.5183 | 66.93649 | 404.3092 | 66.99499 | 464.3191 | 67.34614 |
| 734.5192 | 77.85944 | 474.5595 | 67.82622 | 474.4611 | 67.47656 | 474.2523 | 67.43539 | 474.2625 | 67.74564 |
| 759.3645 | 78.59716 | 484.5121 | 68.49415 | 484.4039 | 67.98909 | 484.1934 | 67.93389 | 484.2049 | 68.36956 |
| 784.2159 | 79.55627 | 494.4462 | 69.49772 | 494.3467 | 68.4022 | 494.1349 | 68.5803 | 494.1476 | 68.76703 |
| 809.0625 | 80.35033 | 504.3979 | 69.36359 | 504.2894 | 68.89189 | 504.0759 | 68.83765 | 504.0904 | 69.38148 |
| 833.9076 | 81.04431 | 514.3369 | 68.45011 | 514.2315 | 69.49242 | 514.018 | 69.47394 | 514.0325 | 69.57954 |
| 858.7516 | 82.33284 | 524.2812 | 69.57912 | 524.174 | 69.88001 | 523.961 | 69.75831 | 523.9743 | 70.03582 |
| 883.5836 | 85.1472 | 534.2184 | 70.70213 | 534.1171 | 70.2414 | 533.9023 | 70.68031 | 533.9129 | 70.42653 |
| 908.4104 | 92.42569 | 544.1627 | 71.30133 | 544.0586 | 70.73646 | 543.8433 | 70.64722 | 543.854 | 70.84563 |
| 933.2436 | 93.97338 | 554.1085 | 71.17789 | 554.0009 | 71.09315 | 553.7827 | 71.27742 | 553.7946 | 71.34044 |
| 968.0719 | 94.6488 | 564.0491 | 71.96126 | 563.943 | 71.30542 | 563.7236 | 71.64352 | 563.7349 | 71.8001 |
| 982.9063 | 94.66073 | 573.9864 | 72.42902 | 573.8845 | 72.05507 | 573.664 | 71.90695 | 573.6743 | 71.9887 |
| 1007.728 | 94.72436 | 583.0346 | 72.96483 | 583.827 | 72.32376 | 583.6039 | 72.20483 | 583.6093 | 72.30099 |
| 1032.55 | 94.79065 | 593.8734 | 73.32114 | 593.7687 | 72.75367 | 593.5441 | 72.60605 | 593.5468 | 72.73835 |
| 1057.382 | 94.87549 | 603.8157 | 73.22173 | 603.7094 | 73.10834 | 603.4845 | 72.89515 | 603.4869 | 73.11959 |
| 1082.196 | 95.59598 | 613.7556 | 73.63943 | 613.6481 | 73.46368 | 613.4229 | 73.26868 | 613.4279 | 73.46839 |
| | | 623.6981 | 74.48619 | 623.5883 | 73.76731 | 623.3625 | 73.58953 | 623.3694 | 73.80164 |
| | | 633.6296 | 74.7224 | 633.5302 | 74.15019 | 633.304 | 73.88605 | 633.3101 | 74.24914 |
| | | 643.572 | 74.78179 | 643.4679 | 74.5895 | 643.2454 | 74.32443 | 643.2497 | 74.43773 |
| | | 653.512 | 75.2015 | 653.4088 | 74.81991 | 653.1891 | 74.53652 | 653.192 | 74.82574 |
| | | 663.4534 | 75.50711 | 663.3503 | 75.05434 | 663.1279 | 74.89317 | 663.1339 | 75.04272 |
| | | 673.3877 | 75.63189 | 673.2905 | 75.38013 | 673.0658 | 75.14174 | 673.0724 | 75.42127 |
| | | 683.3309 | 75.75066 | 683.2297 | 75.69517 | 683.0047 | 75.45988 | 683.0119 | 75.60513 |
| | | 693.2692 | 76.42059 | 693.1683 | 75.97998 | 692.9424 | 75.65239 | 692.9503 | 75.82347 |
| | | 703.2042 | 76.82229 | 703.1056 | 76.17881 | 702.8794 | 75.86448 | 702.8887 | 76.03302 |
| | | 713.1403 | 76.76023 | 713.0451 | 76.50931 | 712.8183 | 76.2191 | 712.8277 | 76.40277 |
| | | 723.0829 | 76.76224 | 722.9828 | 76.93854 | 722.7563 | 76.48658 | 722.7668 | 76.84486 |
| | | 733.0238 | 77.24333 | 732.9222 | 77.20925 | 732.6978 | 76.74934 | 732.7048 | 76.9956 |
| | | 742.9578 | 77.45753 | 742.8615 | 77.48869 | 742.6349 | 77.02425 | 742.6429 | 77.21123 |
| | | 752.9001 | 78.08942 | 752.7985 | 77.82321 | 752.5721 | 77.33091 | 752.5803 | 77.60059 |
| | | 762.8414 | 78.34566 | 762.7341 | 78.15571 | 762.5089 | 77.56732 | 762.5186 | 77.99265 |
| | | 772.7781 | 78.45242 | 772.6708 | 78.43784 | 772.4473 | 77.90708 | 772.4543 | 78.2191 |
| | | 782.7151 | 78.6853 | 782.6067 | 78.62055 | 782.3832 | 78.33194 | 782.3905 | 78.61995 |
| | | 792.6536 | 79.28183 | 792.5468 | 79.12636 | 792.3195 | 78.56295 | 792.327 | 78.88426 |

(Continued)

Appendix 1. Heat capacity data (NATS 58) (Continued)

| T (K) | NATS 58:0 | T (K) | NATS 58:4 | T (K) | NATS 58:8 | T (K) | NATS 58:10 | T (K) | NATS 58:11 |
|---|---|---|---|---|---|---|---|---|---|
| | | 802.5919 | 79.20109 | 802.4853 | 79.18279 | 802.2567 | 78.84259 | 802.2644 | 79.11341 |
| | | 812.5298 | 79.35323 | 812.4236 | 79.65031 | 812.1949 | 79.18843 | 812.2022 | 79.53927 |
| | | 822.4673 | 79.78561 | 822.3631 | 79.96737 | 822.1301 | 79.5113 | 822.1369 | 79.91849 |
| | | 832.4037 | 79.92774 | 832.2966 | 74.25028 | 832.0667 | 79.71529 | 832.0749 | 80.09357 |
| | | 842.3408 | 80.21133 | 842.2325 | 80.7627 | 842.0033 | 79.75582 | 842.0215 | 80.47211 |
| | | 852.2815 | 80.66373 | 852.1697 | 81.27657 | 851.9391 | 80.22594 | 851.9602 | 80.99937 |
| | | 862.2192 | 81.09079 | 862.1047 | 81.6252 | 861.8759 | 81.19455 | 861.8966 | 81.48539 |
| | | 872.1574 | 81.42175 | 872.0428 | 82.26603 | 871.8153 | 81.92 | 871.8329 | 82.19786 |
| | | 882.0962 | 82.14841 | 881.9789 | 83.21182 | 881.7538 | 82.72177 | 881.7632 | 83.16382 |
| | | 892.0324 | 83.38284 | 891.9139 | 84.31413 | 891.6933 | 84.54146 | 891.6966 | 85.94476 |
| | | 901.9711 | 85.02899 | 901.8507 | 87.49007 | 901.631 | 89.28523 | 901.6336 | 90.18376 |
| | | 911.9078 | 88.21785 | 911.7842 | 92.6785 | 911.5666 | 95.2813 | 911.5693 | 92.65307 |
| | | 921.8434 | 92.24213 | 921.7205 | 96.88017 | 921.503 | 93.35624 | 921.5042 | 93.85562 |
| | | 931.7737 | 94.79242 | 931.6562 | 99.74577 | 931.4387 | 96.68559 | 931.4359 | 93.44058 |
| | | 941.7137 | 95.75862 | 941.5929 | 100.8266 | 941.3718 | 95.6393 | 941.3724 | 94.93582 |
| | | 951.6493 | 96.47527 | 951.5292 | 101.0865 | 951.303 | 95.7879 | 951.3067 | 96.4385 |
| | | 961.5875 | 96.61672 | 961.4649 | 101.1148 | 961.2371 | 96.22898 | 961.2402 | 96.24653 |
| | | 971.5181 | 96.39719 | 971.3981 | 101.0496 | 971.1709 | 97.08681 | 971.1725 | 97.2179 |
| | | 981.4554 | 96.80422 | 981.333 | 100.7332 | 981.1029 | 97.18003 | 981.105 | 98.06691 |
| | | 991.3891 | 97.01441 | 991.2663 | 100.6466 | 991.0322 | 97.76363 | 991.0375 | 98.44343 |
| | | 1001.319 | 96.32179 | 1001.2 | 100.3826 | 1000.962 | 97.37051 | 1000.968 | 99.44792 |
| | | 1011.253 | 96.09425 | 1011.138 | 99.84384 | 1010.894 | 99.0801 | 1010.902 | 100.6011 |
| | | 1021.184 | 96.54666 | 1021.074 | 99.83578 | 1020.826 | 100.2649 | 1020.832 | 100.9337 |
| | | 1031.113 | 96.77353 | 1031.004 | 100.619 | 1030.757 | 99.64006 | 1030.763 | 101.461 |
| | | 1041.042 | 96.33647 | 1040.933 | 100.0212 | 1040.682 | 100.9248 | 1040.691 | 101.6381 |
| | | 1050.971 | 96.03687 | 1050.862 | 100.1226 | 1050.609 | 101.4098 | 1050.619 | 102.4736 |
| | | 1060.902 | 96.19434 | 1060.788 | 99.84518 | 1060.538 | 101.1119 | 1060.545 | 102.2363 |
| | | 1070.827 | 96.12695 | 1070.718 | 99.36557 | 1070.466 | 102.6918 | 1070.473 | 102.4634 |
| | | 1080.754 | 95.60515 | 1080.649 | 99.64367 | 1080.395 | 103.6442 | 1080.4 | 102.3032 |
| | | 1090.705 | 95.82935 | 1090.579 | 99.50462 | 1090.324 | 102.4453 | 1090.329 | 103.62 |

Appendix 1. Heat capacity data (NATS 54)

| T (K) | NATS 54:0 | T (K) | NATS 54:6 | T (K) | NATS 54:9 | T (K) | NATS 54:12 |
|---|---|---|---|---|---|---|---|
| 311.927 | 57.487 | 305.278 | 53.557 | 311.921 | 55.391 | 311.931 | 55.792 |
| 336.926 | 59.796 | 315.321 | 55.961 | 336.934 | 58.488 | 336.935 | 58.543 |
| 361.783 | 61.795 | 325.266 | 57.591 | 361.791 | 61.004 | 361.795 | 60.978 |
| 386.639 | 63.426 | 335.210 | 58.807 | 386.646 | 62.797 | 386.652 | 62.701 |
| 411.493 | 65.375 | 345.152 | 59.368 | 411.503 | 64.526 | 411.504 | 64.369 |
| 436.347 | 66.716 | 355.099 | 59.805 | 436.360 | 66.200 | 436.367 | 66.049 |
| 461.198 | 68.162 | 365.044 | 60.669 | 461.215 | 67.702 | 461.218 | 67.541 |
| 486.050 | 69.764 | 374.989 | 61.414 | 486.070 | 69.087 | 486.071 | 68.912 |
| 510.895 | 70.849 | 384.934 | 62.099 | 510.905 | 70.264 | 510.917 | 70.139 |
| 535.748 | 71.966 | 394.879 | 62.838 | 535.757 | 71.396 | 535.760 | 71.306 |
| 560.601 | 73.083 | 404.823 | 63.572 | 560.611 | 72.649 | 560.614 | 72.379 |
| 585.441 | 73.876 | 414.767 | 64.209 | 585.461 | 73.621 | 585.464 | 73.438 |
| 610.293 | 75.145 | 424.712 | 64.948 | 610.317 | 74.568 | 610.318 | 74.266 |
| 635.150 | 75.957 | 434.655 | 65.667 | 635.174 | 75.504 | 635.174 | 75.177 |
| 660.003 | 76.614 | 444.600 | 66.352 | 660.029 | 76.326 | 660.029 | 76.073 |
| 684.854 | 77.458 | 454.544 | 66.873 | 684.874 | 77.096 | 684.873 | 76.787 |
| 709.687 | 78.172 | 464.487 | 67.403 | 709.697 | 77.860 | 709.704 | 77.487 |
| 734.512 | 78.846 | 474.430 | 68.012 | 734.532 | 78.538 | 734.530 | 78.155 |
| 759.359 | 79.821 | 484.373 | 68.409 | 759.376 | 79.261 | 759.375 | 78.893 |
| 784.200 | 80.489 | 494.317 | 69.019 | 784.226 | 79.954 | 784.215 | 79.647 |
| 809.048 | 81.242 | 504.259 | 69.609 | 809.074 | 80.913 | 809.064 | 80.354 |
| 833.893 | 81.594 | 514.201 | 70.202 | 833.922 | 81.524 | 833.910 | 81.013 |
| 858.738 | 82.259 | 524.144 | 70.347 | 858.766 | 82.459 | 858.758 | 81.928 |
| 883.580 | 83.107 | 534.084 | 70.875 | 883.606 | 83.935 | 883.600 | 83.385 |
| 908.419 | 84.272 | 544.024 | 71.496 | 908.434 | 87.089 | 908.423 | 86.242 |
| 933.247 | 87.387 | 553.966 | 71.931 | 933.268 | 88.040 | 933.255 | 86.535 |
| 958.078 | 93.808 | 563.908 | 72.206 | 958.097 | 93.105 | 958.088 | 91.014 |
| 982.909 | 95.117 | 573.850 | 72.624 | 982.927 | 95.267 | 982.916 | 93.099 |
| 1007.737 | 95.799 | 583.793 | 72.935 | 1007.754 | 99.415 | 1007.743 | 97.644 |
| 1032.565 | 95.954 | 593.734 | 73.441 | 1032.580 | 101.842 | 1032.571 | 100.779 |
| 1057.391 | 96.286 | 603.674 | 73.718 | 1057.407 | 104.815 | 1057.394 | 103.148 |
| 1082.210 | 96.212 | 613.616 | 74.026 | 1082.229 | 105.041 | 1082.211 | 103.501 |

(Continued)

Appendix 1. Heat capacity data (NATS 54) (Continued)

| T (K) | NATS 54:0 | T (K) | NATS 54:6 | T (K) | NATS 54:9 | T (K) | NATS 54:12 |
|---|---|---|---|---|---|---|---|
| | | 623.556 | 74.313 | | | | |
| | | 633.494 | 74.702 | | | | |
| | | 643.430 | 74.989 | | | | |
| | | 653.371 | 75.247 | | | | |
| | | 663.309 | 75.678 | | | | |
| | | 673.250 | 75.815 | | | | |
| | | 683.190 | 76.060 | | | | |
| | | 693.129 | 76.308 | | | | |
| | | 703.066 | 76.523 | | | | |
| | | 713.005 | 76.629 | | | | |
| | | 722.945 | 76.927 | | | | |
| | | 732.882 | 77.251 | | | | |
| | | 742.820 | 77.454 | | | | |
| | | 752.758 | 77.737 | | | | |
| | | 762.695 | 78.038 | | | | |
| | | 772.632 | 78.242 | | | | |
| | | 782.571 | 78.448 | | | | |
| | | 792.509 | 78.677 | | | | |
| | | 802.448 | 78.842 | | | | |
| | | 812.387 | 79.312 | | | | |
| | | 822.326 | 79.310 | | | | |
| | | 832.260 | 79.613 | | | | |
| | | 842.197 | 79.382 | | | | |
| | | 852.134 | 80.303 | | | | |
| | | 862.071 | 80.450 | | | | |
| | | 872.004 | 80.794 | | | | |
| | | 881.941 | 81.126 | | | | |
| | | 891.878 | 81.700 | | | | |
| | | 901.816 | 82.238 | | | | |
| | | 911.753 | 83.067 | | | | |
| | | 921.690 | 85.127 | | | | |
| | | 931.627 | 88.045 | | | | |
| | | 941.563 | 90.882 | | | | |
| | | 951.500 | 93.327 | | | | |
| | | 961.433 | 95.219 | | | | |
| | | 971.365 | 95.033 | | | | |
| | | 981.297 | 94.527 | | | | |
| | | 991.229 | 94.190 | | | | |
| | | 1001.159 | 94.281 | | | | |
| | | 1011.091 | 94.829 | | | | |
| | | 1021.020 | 94.808 | | | | |
| | | 1030.951 | 95.678 | | | | |
| | | 1040.881 | 95.696 | | | | |
| | | 1050.808 | 96.495 | | | | |
| | | 1060.737 | 94.940 | | | | |
| | | 1070.664 | 97.186 | | | | |
| | | 1080.592 | 99.755 | | | | |
| | | 1090.521 | 99.977 | | | | |